Experimental study on the influence of bed protections on scour depth and scour development in front of sloped embankments.

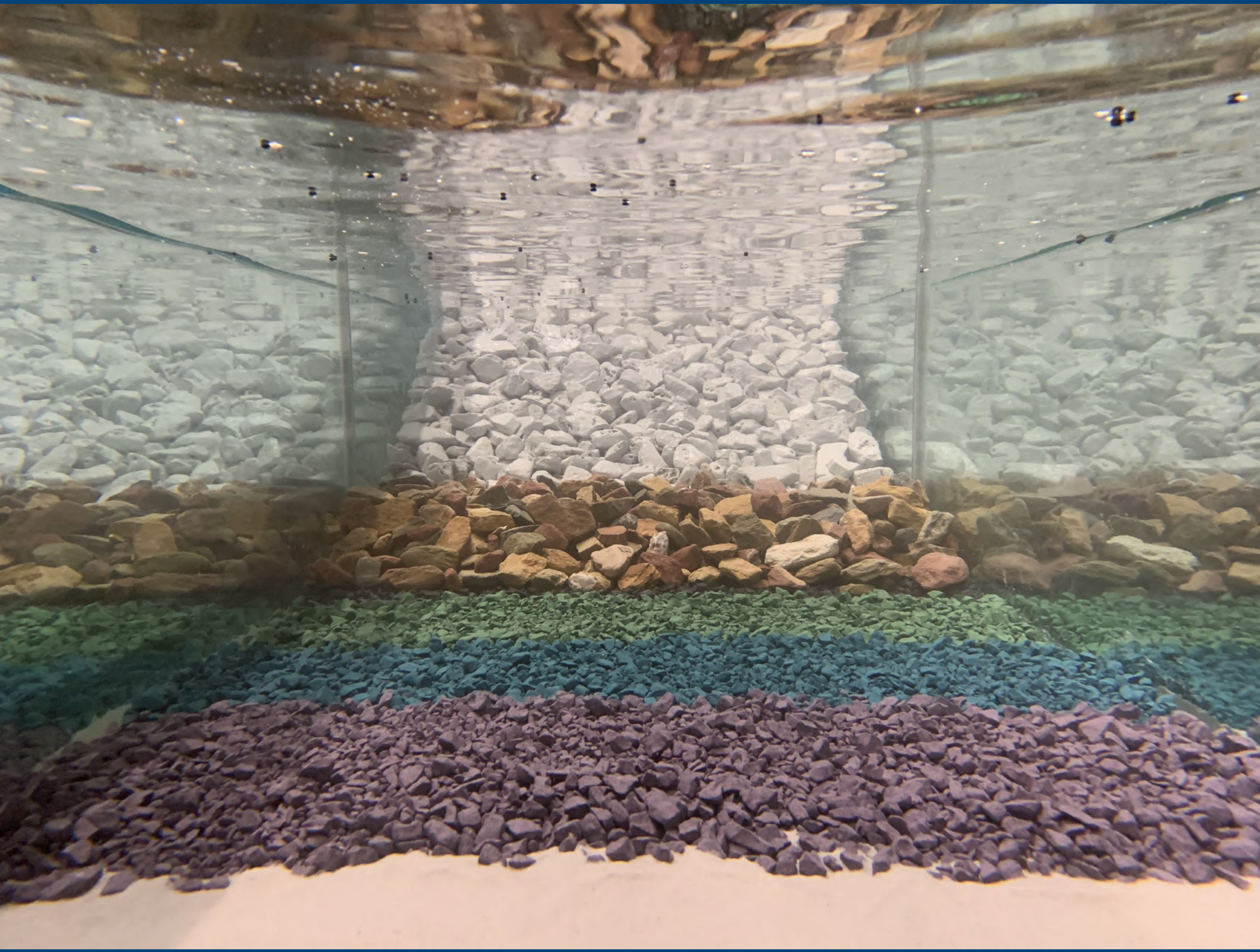

Casper Jantzen

Experimental study on the influence of bed protections on scour depth and scour development in front of sloped embankments.

by

C.F. Jantzen

To obtain the degree of Master of Science in Hydraulic Engineering

at the Delft University of Technology,

to be defended publicly on October 28, 2020 at 14:30.

This study was part of the project Labwerk Coastal Structures (LabCoSts),
which is supported by TKI Deltatechnologie.

Graduation Committee:	Dr. ir. B. Hofland	TU Delft
	ir. C. Kuiper	TU Delft
	Dr. ir. M. A. de Schipper	TU Delft
	ir. W. J. Ockeloen	Van Oord

Preface

Ten months ago I started working on my thesis as a completion of my master in Hydraulic Engineering at the TU Delft. As a graduation intern at Van Oord, I was given the opportunity to get to know a great company in the coastal engineering sector. This paper is the result of a project in which, I started researching the scour in front of sloping breakwaters. I chose this project because it included physical scale model tests in the wave flume of the university. This was something I preferred as opposed to numerical modelling, as it meant I did not have to sit at a desk for an entire year. Instead, I had the opportunity to perform interesting and also fun experiments to enlarge the knowledge on scour.

To execute the physical model tests, I had to make a design, build the experiment set-up and perform the tests. The schedule was quite tight, resulting in a somewhat busy preparation period. The Corona pandemic threw a spanner in the schedule and resulted in a delay of the delivery of the breakwater structure. Since the wave flume was already available and the rest of the set-up placed inside the wave flume, the decision was made to perform tests on an impermeable slope/ embankment. However, also due to the Corona pandemic, the wave flume was available for a longer period of time, thus the original planned tests on a permeable breakwater could also still be performed. This extended the research from just breakwaters to sloped embankments, both permeable and impermeable.

Thanks to the flexibility of everyone involved, I was able to execute my research at the university while our country was in an "intelligent lockdown". For this I am very grateful to my graduation committee, my roommates and most of all the staff members of the fluid dynamics laboratory. They helped me build and place all the needed components to perform the experiments, for which I would like to thank them.

At the same time, I could not have achieved this without everyone who supported me. First of all, I had two dedicated daily supervisors who advised and guided me with their expertise in physical modelling and coastal structures. Wouter Ockeloen working at Van Oord and Coen Kuiper working at the TU Delft who reviewed my written report in great detail. My other colleagues at Van Oord also functioned as valuable discussion partners and gave me the opportunity to perform a practice presentation.

Furthermore, Bas Hofland who, as my professor and the chairman of the graduation committee, contributed especially by enabling me to perform the tests that I wanted to do in the wave flume. Besides that, his endless enthusiasm would keep anyone motivated while working in the fluid dynamics laboratory. Also Matthieu de Schipper, who is my external TU Delft committee member, contributed with his knowledge in sediment transport.

Additionally, I want to thank all my friends who contributed to my research, report or presentation. Their contributions varied from reading one page to multiple chapters and from drawing a grid on the wave flume to preparing my online presentation zoom session. Nonetheless I would like to thank all of them: Aman Singhvi, Ella Scheltinga, Ron Bruijns, Nikita Ham, Gerrit de Leeuw, Jesse van den Berg, Wisse Goedhart, Madelief Doeleman, Martine Rottink and Anoushka Verhoeven.

Finally, I would like to thank my family for their support during all these years of studying. And last but not least, you and everyone with you, who is reading my report.

Thank you all for your unwavering support.

Casper Jantzen
Delft, October 2020

Abstract

On the seabed in front of coastal structures sediment movement takes place due to incoming waves. The erosion of sediments creates a scour hole at the toe of structures such as embankments, breakwaters and dikes. This scour hole may lead to instabilities in the main structure due to material sliding into this hole. A common method of protecting against scour is the placement of a rubble mound toe structure and bed protection. The goal of this study is to better understand the background and main parameters that leads to scour, to predict the (location of the) maximum scour depth and how this is influenced by the bed protection. Consequently, the main research question of this thesis is: *What is the expected, wave induced, scour depth over time in front of a sloped embankment, and what is the effect of a scour protection on the (location of the) maximum scour depth?*

Small scale physical model tests were performed in the wave flume of the Civil Engineering fluid dynamics laboratory at the TU Delft, to obtain data on scour in front of an embankment. The embankment was modelled as a structure with a 1:2 slope with a sandy bed in front of it. On the bed a toe structure and bed protection were placed, consisting of stable rock layers and a filter layer under the toe to prevent winnowing. In these model tests the permeability of the embankment, the bed protection length and the hydraulic conditions were varied. The obtained data from flume tests were supplemented by findings from prior studies to characterise the formation of scour.

It followed from the analysis that multiple processes have an influence on the amount of scour. These processes can be described as: downrush flow, standing wave pattern, undertow, asymmetric waves and ripples. The two most important processes are the standing waves and the downrush flow. Furthermore, the analysis showed that the bed protection length directly influences the location of the scour hole. This is caused by the downrush flow, which influences the erosion pattern directly in front of the bed protection. However, the maximum depth of the scour hole is barely influenced by the amount of bed protection.

In contrast to the bed protection, the permeability of the structure and the hydraulic conditions have large influences on the amount of scour. This followed from the findings that the degree of reflection is an essential parameter, which depends on the hydraulic conditions and the permeability of the structure. The findings are used to derive eq. (1), which estimates the maximum scour depth development over time. Equation (2), shows the scour pattern, based on the node and anti-node pattern close to the coastal structure. For the downrush flow scour a positive linear dependency in relation to the permeability of the embankment was found. Furthermore, a longer bed protection decreases scour due to downrush flow. However, a quantitative relation for downrush flow scour was not found.

$$\frac{S(N)_{max}}{H_s} = \frac{0.3}{(\sinh\frac{2\pi h}{L_p})^{1.35}} K_r^2 \sqrt{\frac{N}{N_0}} \tag{1}$$

$$\frac{S(x,N)}{H_s} = \frac{0.3}{(\sinh\frac{2\pi h}{L_p})^{1.35}} e^{(-\frac{0.85x}{L_p})} \cos(\frac{4\pi x}{L_p}) K_r^2 \sqrt{\frac{N}{N_0}} \tag{2}$$

$S(x,N)$ = Scour, $S(N)_{max}$ = Maximum scour, N = number of waves, N_0 = 12000, x = Distance from embankment, H_s = Significant wave height, h = Water depth, L_p = Peak wavelength K_r = Reflection coefficient.

Therefore, the conclusion and answer to the main research question of this study is: The expected wave induced scour in front of a sloped embankment can be approximated by eq. (1). The effect of the bed protection on the maximum scour is negligible. The location of the scour changes for different bed protection lengths, which can be relevant for the design of structures. Furthermore, the essential parameters to determine the scour pattern are the reflection coefficient and the local peak wavelength. For further research it is recommended to validate the proposed equations on various hydraulic conditions. Besides that, extra tests can be performed to derive a quantitative relation, with observance of the bed protection, for the downrush flow scour.

Contents

List of symbols

a	$[m]$	Wave amplitude
a_b	$[m]$	Wave amplitude at the bottom
C	$[-]$	Chezy coefficient
c_f	$[-]$	Friction coefficient
Ca	$[-]$	Cauchy number
d	$[m]$	Grain diameter
d_n	$[m]$	Nominal grain diameter
$d_n x$	$[m]$	Nominal grain diameter where x% of the grain mass has a smaller diameter
$d*$	$[-]$	Dimensionless grain diameter
d_{n50}	$[m]$	Median nominal grain diameter
D	$[h]$	Test duration
Fr	$[-]$	Froude number
g	$[m/s^2]$	Acceleration of gravity
h	$[m]$	Water depth at toe
h_0	$[m]$	Offshore water depth
h_t	$[m]$	Water depth on top of toe structure
H	$[m]$	Wave height
H_s	$[m]$	Significant wave height (Hm0)
k	$[1/m]$	Wave number
k_r	$[m]$	Roughness of bottom
K_R	$[-]$	Reflection coefficient
L	$[m]$	wavelength (local)
L_p	$[m]$	Peak wavelength (local)
n	$[-]$	Scale factor
N	$[-]$	Number of waves
N_{OD}	$[-]$	Number of damage: Number of displaced stones per stone width.

P	$[-]$	1. Permeability
	$[-]$	2. Rouse number
R	$[m]$	Hydraulic radius
Re	$[-]$	Reynolds-number
$Re*$	$[-]$	Particle Reynolds-number
$s_{o,p}$	$[-]$	Offshore wave steepness
S	$[m]$	Scour depth
S_d	$[-]$	Damage number for van der Meer
t	$[m]$	Thickness
T	$[s]$	Wave period
$T_{m-1,0}$	$[s]$	Mean spectral wave period
T_p	$[s]$	Peak period of wave spectrum
u	$[m/s]$	Velocity in x-direction
$u*$	$[m/s]$	Shear velocity
$u*_c$	$[m/s]$	Critical shear velocity
$\bar{u}$	$[m/s]$	Depth averaged velocity
u_b	$[m/s]$	Velocity at the bottom
$\hat{u}$	$[m/s]$	Maximum velocity
We	$[-]$	Weber number
W_bp	$[m]$	Bed protection width
W_t	$[m]$	Toe width
w_s	$[m/s]$	Sediment fall velocity
z	$[m]$	Distance along x-axis
α	$[-]$	Slope angle
Δ	$[-]$	Relative density
γ	$[-]$	Roughness factor
κ	$[-]$	Von Kármán constant
ν	$[m^2/s]$	Kinematic viscosity
ρ_s	$[kg/m^3]$	Density of solids
ρ_w	$[kg/m^3]$	Density of water
σ	$[N/m]$	Surface tension
τ	$[N/m^2]$	Shear stress
τ_c	$[N/m^2]$	Critical shear stress

τ_w	$[N/m^2]$	Shear stress under oscillatory flow (waves)
ψ	$[-]$	Shields mobility parameter
ψ_c	$[-]$	Shields stability parameter
ω	$[1/s]$	Angular frequency in waves
ξ	$[-]$	Irribarren number

Chapter 1

Introduction

This chapter introduces the topic of this research. Firstly, in section 1.1 coastal defence structures and the phenomenon scour in front of these structures are discussed. Secondly, the problem is described in section 1.2. The research questions of this study are formulated in section 1.3. Finally, the methodology and the report layout are discussed in section 1.4.

1.1 Background

For centuries people have been building structures in or close to the water. Many of these structures are designed to keep infrastructure, cities and people safe. In this research the focus lies on coastal defence structures such as sloping breakwaters, revetments and dikes. These structures have the essential function of breaking waves coming in from the sea to create sheltered waters and dry land. In fig. 1.1 the breakwater of Mackay harbour can be seen. This conventional rubble mound structure shelters the marina from the incoming waves. In this case, it can be seen that the outer armour layer consists of large stones. In other designs multiple different outer layers are used.

Figure 1.1: Conventional rubble mound breakwater. *Location: Mackay (Australia)*

This is however only a small part of the rubble mound structure, most of it is below the water surface and can not be seen. In this specific breakwater the inner and outer armour layer together with the crest can be seen. The filter layer, core, toe structure and the bed protection are below the water surface. For all coastal structures large parts are built below the water surface and therefore the interaction between the structure and the water is vital to understand. The understanding of coastal defence structures and their surroundings ensures their stability and endurance.

The different parts and aspects of coastal defence structures could fail in various ways. For a rubble mound structure mechanisms such as overtopping, slip failures, toe erosion, berm erosion and much more could lead to the failure of a rubble mound structure. A summary of the failure modes of a conventional breakwater can be found in fig. 1.2. These are similar for most rubble mound structures, but for dikes or seawalls the failure mechanisms differ in certain aspects. In this thesis, the failure mechanism of toe scour and seabed scour close to the toe structure are researched for sloping dikes, revetments and breakwaters. In front of all these kinds of structures scour occurs due to incoming and reflecting waves.
Scour is the process of eroding bed material, since coastal structures are often built on sand or clay this is an important issue. Scour can cause the coastal structure to become unstable, at a breakwater a scour hole could form in front of the toe structure which would undermine the breakwater stability. Thus, scour could cause instabilities in the lower regions of the structure which may eventually lead to instabilities in the whole structure. Although revetments and dikes have differences compared to a breakwater, they do have similar scour protections. Often a toe structure and a bed protection are used to prevent scour due to waves, this will be discussed in more detail in chapter 2.

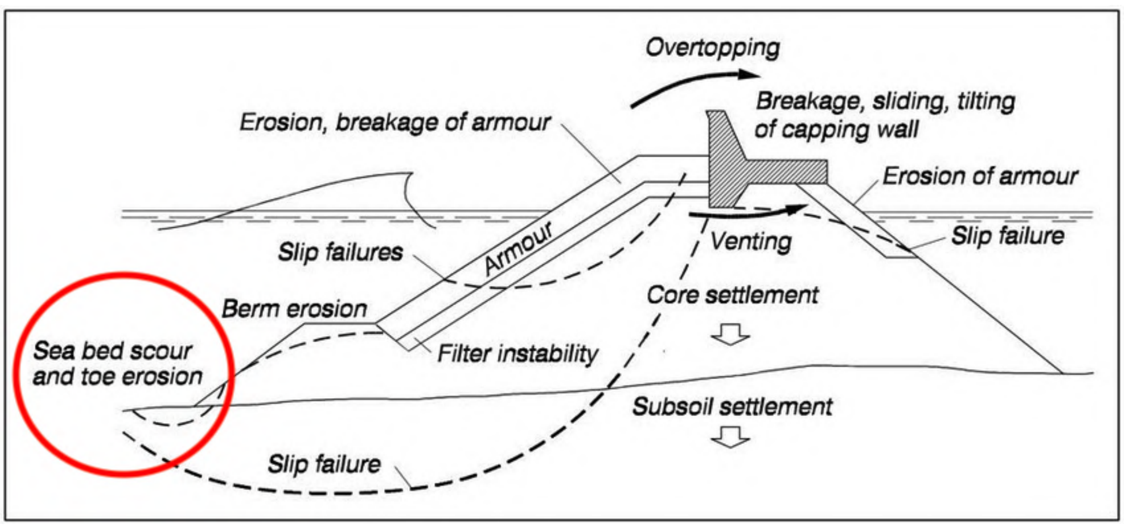

Figure 1.2: Failure modes of a conventional breakwater. Tulsi (2016)

1.2 Problem description

All structures built in moving water on a soft soil such as clay, sand or gravel often induce scour in the surrounding bed. Scour can lead to instability of structures and is thus an important failing mechanism to consider and understand. As described in section 1.1 the toe structure and a bed protection are used to prevent scour in front of breakwaters, revetments and dikes. In the field of coastal engineering many empirical formulas already exist for the design of coastal defence structures. These formulas cover important aspects such as stability, overtopping, run-up and more. For toe scour however, only estimations and rules of thumb are given in guidelines such as the Rock Manual. Since numerical models do not yet provide reliable data or calculations and there is not enough physical data available more research is still needed. This research would aid in more accurately predicting the amount of scour so that designs of breakwaters, revetments and dikes can be further improved.

1.3 Research questions

The main goal of this study is to characterise the maximum scour depth and scour development over time in front of the toe structure of sloped embankments and how this is influenced by the bed protection in front of the structure. Consequently, the main research question is:

What is the expected, wave induced, scour depth over time in front of a sloped embankment, and what is the effect of a scour protection on the (location of the) maximum scour depth.

To answer this question a few sub questions are formulated:

- Which parameters have an influence on scour in front of the toe structure of a sloped embankment and how are the parameters related to the scour?
- What is the effect of permeability of the structure on the scour depth?
- What is the influence of a toe/bed protection on the scour in front of a sloped embankment?
- What is the equilibrium depth for a scour hole in front of a sloped embankment and which variables influence this?
- From which point in the structure or scour protection should the length of the total bed protection be measured?*
- Which wave period should be used to determine the wavelength and derive corresponding scour patterns?*
- Given the main objective of the research, how can a sand bed be modelled most accurately in a small scale model?

** An important assumption is whether the distance to the end of the scour protection is measured from the toe of the structure, the intersection of the waterline and the structure or another location. This location also indicates the total length of the scour protection. Besides that, the length of the scour protection is partially based on nodes and anti-nodes, which are related to the wavelength. The wavelength is based on the wave period which can be a peak period, mean period or another wave period parameter. Thus, to relate scour patterns and parameters, the correct parameters must be chosen and presented. Especially important is the definition of the bed protection length in combination with the wavelength.*

1.4 Methodology

To answer the mentioned research question, data on scour in front of the toe structure has to be obtained. This is done by performing – small scale – physical modelling tests. The obtained data is analysed to give relations between scour and the researched parameters. In order to execute the physical model tests, a number of different steps have to be taken. In the remainder of this section, the structure of the report is described which is in line with the steps executed during the research project.

First of all, the literature study is presented in chapter 2. Important aspects such as structure dimensions, sediment movement, scour due to waves, parameter analyses and scaling laws are discussed. The knowledge obtained from the literature study is used to make considerations and assumptions for the experiment set-up and the test program. Furthermore, it is also used to analyse the test results and draw conclusions from them.

In this research physical scale model tests are used to collect data. Tests are done and data is collected on two different structure types. First of all, tests are done on an impermeable smooth slope corresponding to for instance a dike. Secondly, tests on a permeable and rough rubble mound slope are executed, which is the main focus of this research. In chapter 3 the experiment set-up is described. This includes the test facilities, the physical model set-up and the measurement devices. This also includes the design of the physical model and partly the construction of it.

There are multiple parameters which have an influence on scour. The parameters varied in this research are limited to the length of scour protection, the permeability of the coastal defence structure and the wave conditions. In chapter 4 it is explained why these parameters have been varied. Besides that, the used hydraulic conditions and structure configurations are discussed. In short, chapters 3 and 4 contain the information needed to recreate the experimental procedure in exactly the same way as this research.

Chapter 5 contains the results and observations of the physical model tests. This is followed by the analysis, in chapter 6, which is done on the collected data. In this the results are used and related to existing literature in addition to the provided new insights. The analysis and the results are discussed in chapter 7. The conclusions and the answers to the research questions are stated in chapter 8 and finally recommendations can be found in chapter 9.

Chapter 2

Literature research

This chapter reviews the available literature to get an understanding of what is already known in this field of research. First of all, in section 2.1 the basic concepts of sediment transport are explained in uniform flow and in waves. Secondly, in section 2.2 the layout and stability of sloped embankments and the theory behind the designs are discussed. The knowledge of these two sections is needed to understand the concept of scour in front of breakwaters or revetments, this is described in section 2.3. In section 2.5 a list of parameters of influence to the problem is presented. The chapter is concluded in section 2.4 with the applicable scaling laws when comparing small scale with full scale.

2.1 Sediment transport

Sediment transport is the movement of solid particles in a fluid, being in this case water. In oceans sediment is mainly transported by tidal and wave induced currents. For coastal structures sediment transport can be caused by small scale motions of individual waves and larger scale motions by wave groups or tidal induced currents. Both are important for coastal structures however, for this research only the cross-shore sediment transport due to waves is considered. The transport of sediment is initiated when the movement of water is exerting a frictional force on the grains bigger than the retaining force. The retaining force is the combined force of the gravitational force and the friction between the grain and the surrounding grains.

In uniform flow this initiation of motion happens when the flow velocity is larger than the critical velocity, which is defined as the velocity when the grain or grains start to move. Two approaches can generally be used to determine if there is sediment movement, namely the Izbash approach or the Shields approach. Izbash considers forces on individual grains and tries to balance these forces, while Shields considers the friction force caused by the water on the bed; Schiereck and Verhagen (2012). Izbash is more accurate to use when the water depth is small compared to the grain size while Shields is more accurate when the water depth is large compared to the grain size. Scour is the process of eroding bed material. In general, the bed material has a small grain compared to the water depth, thus Shields should be used. Shields can also be used to investigate if the bed protection is stable, which usually also contains quite small grains compared to the water depth. Thus, to determine if scour will occur and if the bed protection is stable, Shields formula is used.

2.1.1 Shields

The Shields formula originates from Shields (1936) and the formula gives a relation between the dimensionless shear stress and the particle Reynolds-number, this relation can be seen in eq. (2.2). The Shields parameter is also described and explained in many books and guidelines such as the *Rock Manual* by Dont and Laborie (2007) and *Introduction to bed, bank and shore protection* by Schiereck and Verhagen (2012). In eq. (2.1) the Shields parameter is expressed as this dimensionless shear stress. The shear stress is related to the density of the fluid multiplied by the shear velocity squared. Thus, the Shields parameter can be described as the shear velocity, relative density, acceleration of gravity and the grain diameter. When the subscript 'c' is used, the shields parameter is a stability parameter since it indicates the critical value for the velocity for which the grains start to move. If the actual velocity or the actual shields parameter is used, thus without the subscript, it is a mobility parameter. So, if the actual velocity is larger than the critical velocity sediment transport occurs, the same holds for the critical shear stress and shear stress. Figure 2.1 shows that, everything below the line is stable and everything above the line is unstable.

$$\psi_c = \frac{load}{strength} = \frac{\tau_c d^2}{(\rho_s - \rho_w) g d^3} = \frac{\tau_c}{(\rho_s - \rho_w) g d} = \frac{u*_c^2}{\Delta g d} \tag{2.1}$$

$$\psi_c = f(Re*) \tag{2.2}$$

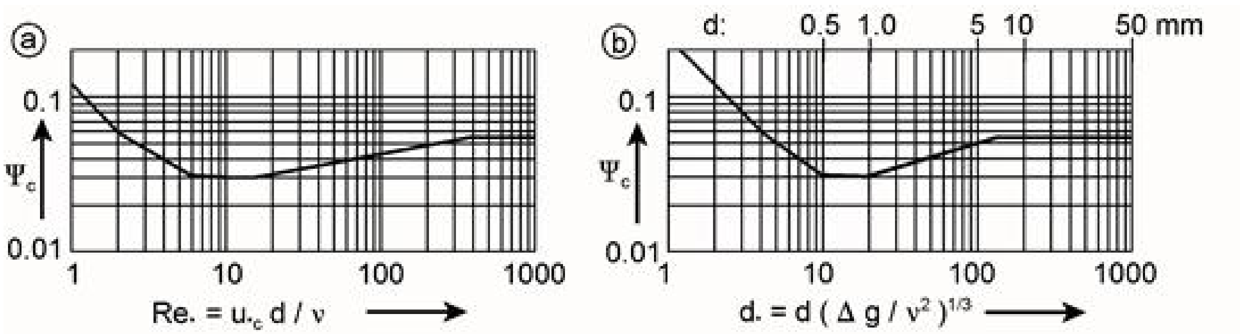

Figure 2.1: Critical shear stress according to Shields – van Rijn. Schiereck and Verhagen (2012)

Figure 2.1 indicates that according to Shields parameter, for grains larger than $7mm$ the value for the Shields parameter is constant ($\psi_c = 0.055$). However, when the grains are smaller the value is not constant and iteration with the diameter is often needed. This is clearly seen in the right graph of fig. 2.1. For smaller diameters ψ_c is not constant and since ψ_c changes with the grain diameter iteration is needed. It gets more difficult if the definition of the Shields parameter and the shear stress are considered more closely. The definition of motion can be interpreted in many different ways since the Shields parameter considers the whole bed structure. Therefore, if one particle is moving it is not necessarily considered as movement.

In fig. 2.2 the different definitions of motion are formulated. Shields parameter can be found between 'frequent particle movement at all locations' and 'permanent movement at all locations'. Since the Shields parameter is not a physical parameter but a value found by curve fitting it has a standard deviation and a mean. Thus the constant value in fig. 2.1 is an arbitrary number and is actually a range. The Rock Manual, Dont and Laborie (2007), recommends for limited movement a value of ψ_c between $0.05 - 0.055$ and for when the first stones start moving ψ_c between $0.03 - 0.035$. Thus, the different stages of movement actually have a probability of being exceeded according to Schiereck and Verhagen (2012). This definition also holds for the critical shear stress which, when exceeded by the actual shear stress also insinuates movement. If then the actual shear stress is considered, another definition problem arises.

The actual shear stress is defined in eq. (2.3) and depends on the density of water, the acceleration of gravity, the mean velocity of the water column and the Chezy coefficient. The Chezy coefficient, eq. (2.4), in turn depends on the hydraulic radius and the factor k_r which is a definition for the roughness of the bed. Often k_r is defined the d_{n50} of the bed material multiplied with a constant, researchers did not find a single number. A range between 2 d_{n50} to 6 d_{n50} is proposed dependent on the application and on the chosen factor of ψ_c. The Rock Manual proposes to choose a practical value of 4 d_{n50} which corresponds to the ψ_c between $0.05 - 0.055$. Schiereck and Verhagen (2012) proposes a practical value of 2 d_{n50} which corresponds to $\psi_c = 0.03$. Both propositions give similar results when used in practise, but they only hold

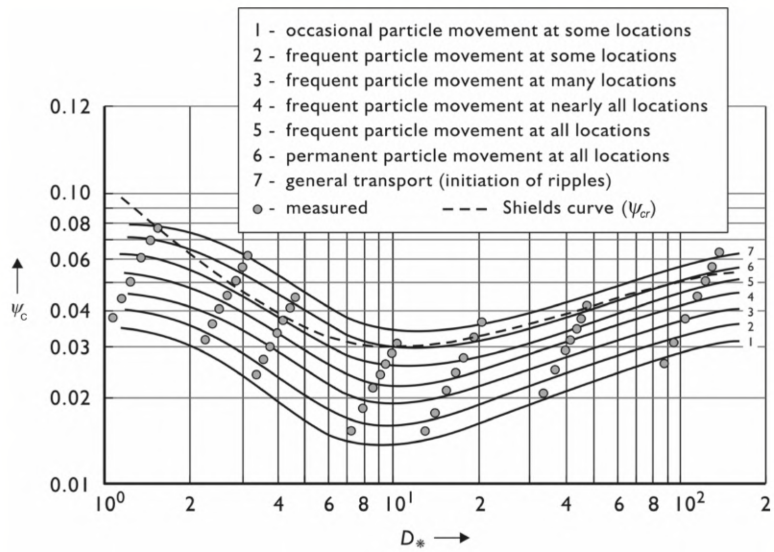

Figure 2.2: Shields diagram and definition of motion. Dont and Laborie (2007)

for grain sizes above the earlier mentioned $7mm$. For the original Shields curve as shown in fig. 2.1, it is more appropriate to use the value of 4 d_{n50} since this corresponds to the values between $0.05 - 0.055$, the original Shields curve also falls between this range.

$$\tau = \rho_w g \frac{\bar{u}^2}{C^2} \tag{2.3}$$

$$C = 18 log\left(12\frac{R}{k_r}\right) \tag{2.4}$$

The diagrams and formulas presented in this section can be used to determine if a bed protection or a sand-bed is stable. When the hydraulic conditions are known the minimum grain diameter can be determined. Or if the grain size is known, the maximum allowable conditions can be derived. However, this is limited to uniform flow and does not consider waves. The next section explains how to use Shields equation when waves are present. For scour due to waves some additional aspects need to be considered. First of all, sediment transport in non breaking waves will discussed using a modified version of Shields, namely Sleath.

2.1.2 Modified Shields (Sleath)

For non-breaking waves sediment transport is fairly similar in theory compared to Shields, the shear stress can still be used to determine the stability of the bed material. However, the shear stress is calculated in a different manner since the flow is not uniform but oscillatory. For stability the maximum shear stress must be considered, this is defined for waves in eq. (2.5). The shear stress is still related to the (maximum) velocity squared and the density of water. In contrast to the shear stress, the friction coefficient is defined differently. This is because the Chezy coefficient, $c_f = g/C^2$ for uniform flow, can not be used and thus a different formulation is used. Equation (2.6) gives the empirical formula based on measurements for friction under waves. A simplified and more practical form, eq. (2.7), is used by Schiereck and Verhagen (2012) and Dont and Laborie (2007). The simplified form has limitations and thus a maximum friction coefficient of $c_f = 0.3$ is usually considered.

$$\hat{\tau}_w = \frac{1}{2}\rho_w c_f \hat{u}_b^2 \tag{2.5}$$

$$c_f = e^{-6+5.2(a_b/k_r)^{-0.19}} \tag{2.6}$$

$$c_f = 0.237\left(\frac{a_b}{k_r}\right)^{-0.52} \quad \text{for} \quad a_b > 0.636k_r \tag{2.7}$$

Another difference between Shields and Sleath is the used velocity. Since the velocity is not uniform a maximum velocity at the bottom is needed to determine the shear stress. The maximum velocity at the bottom can be determined by using the wave characteristics as shown in eq. (2.8). This can be simplified to eq. (2.9) since the maximum velocity implies $\sin(\theta) = 1$ and at the bottom implies $h + z = 0$ and thus also $\cosh\big(k(h+z)\big) = 1$.

$$u = \omega a \frac{\cosh\big(k(h+z)\big)}{\sinh(kh)} \sin(\theta) \tag{2.8}$$

$$\hat{u}_b = \frac{\omega a}{\sinh(kh)} \tag{2.9}$$

Although the shear stress can now be calculated and all parameters are known to use the Shields approach results differ from the original Shields curve. In fig. 2.3 both curves are plotted and it is evident that especially for lower values of the dimensionless particle diameter a lower stability parameter is found. For the higher dimensionless particle diameters the value for ψ_c is around 0.055 to 0.056, which is equal to Shields for uniform flow.

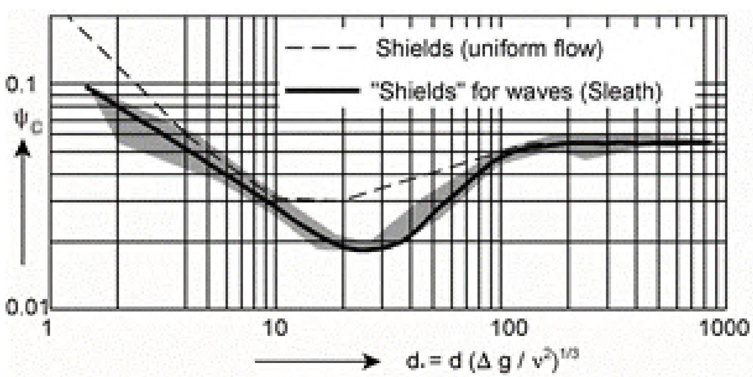

Figure 2.3: Sleath: Shields for waves. Schiereck and Verhagen (2012)

2.2 Sloped embankments

For the physical tests, a scale model was made. In order to do that basic knowledge of breakwaters, dikes and revetments is needed. Although the focus lies on the scour in front of the toe structure the upper part of the structure also influences the amount of scour. For the remainder of this thesis dikes, revetments and breakwaters will be referred to as a sloped embankments which, can be classified as either permeable or impermeable and smooth or rough. Design factors such as permeability and smoothness have a considerable influence on the reflection. This will be explained in more detail in section 2.3.

To understand the problem of scour in front of the toe structure, it is first important to understand the construction and the design of a sloped embankment. In fig. 2.4 a conventional cross section of a breakwater, dike or revetment can be seen. The structure itself often consists of a core, a filter layer and an armour layer. The core is built on the seabed and defines the shape of the embankment. Depending on the function of the structure, the core can be made out of sand or quarry run for permeable structures and clay for impermeable structures. The armour layer consists of large stones or concrete units which absorb the impact of the waves. These armour units are available in many different forms and have a large influence on the roughness of the slope and the reflection of the waves.

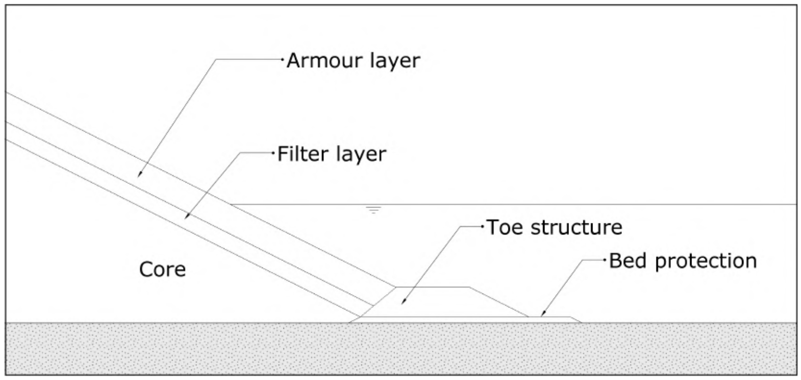

Figure 2.4: Cross section of a sloped embankment.

In most cases, the armour layer is supported by a toe structure to prevent the armour layer from sliding down. The toe is constructed of large stones and it also protects the bottom from the downrush flow of the incoming waves. When a toe structure is directly built upon a sand layer, a phenomenon known as winnowing has a large probability of occurring. Due to the large difference in grain size between the stones and the sand, the water-flow causes the sand to flow upwards trough the pores of the stones. If this process continues over an extended period of time, the toe structure sinks into the sand and may eventually cause instabilities. This is why a filter layer, consisting of smaller stones, between the toe structure and the sand is used.

Finally, at the most seaward part of the structure, a scour protection can placed. This protects the bottom from erosion that would have been caused by the water flow of the incoming and reflecting wave. The bed protection and the filter layer underneath the toe structure can often be combined, as is done in fig. 2.4. These last two aspects, the toe structure and the bed protection, are the main focus of this research. Their influence will further be discussed in section 2.3.

Thus, the armour layer and filter layer are different for dikes, revetments and breakwaters. While the toe structure and bed protection are similar for all cases. When assuming a sandy bed, a filter layer and a toe structure are used to protect the sand bed from eroding in front of these structures. In other words, the same defence mechanism against scour is used for all structures. This is why all kind of embankments, such as dikes, revetments and breakwaters, can be considered in this research.

2.3 Wave induced scour in front of sloped embankments

Scour in front of sloped embankments occurs due to the interaction between the incoming waves, the structure and the seabed. There are two main causes of scour at sloped embankments, which are:

- The downrush flow of the breaking or surging wave along the slope having a direct impact on the bed just in front of the structure.
- A standing wave pattern caused by incoming and reflecting waves creating ripples in the bed with a length scale of half a wavelength, as shown in fig. 2.5.

These mechanisms of scour in front of structures are already understood quite well. This was first systematically researched for vertical walls by Xie (1981) and for rubble mound structures by Sumer and Fredsøe (2000). The difference in scour between vertical walls and rubble mound structures is mainly caused by the difference in reflection coefficient. When waves are fully reflected the standing wave pattern has the

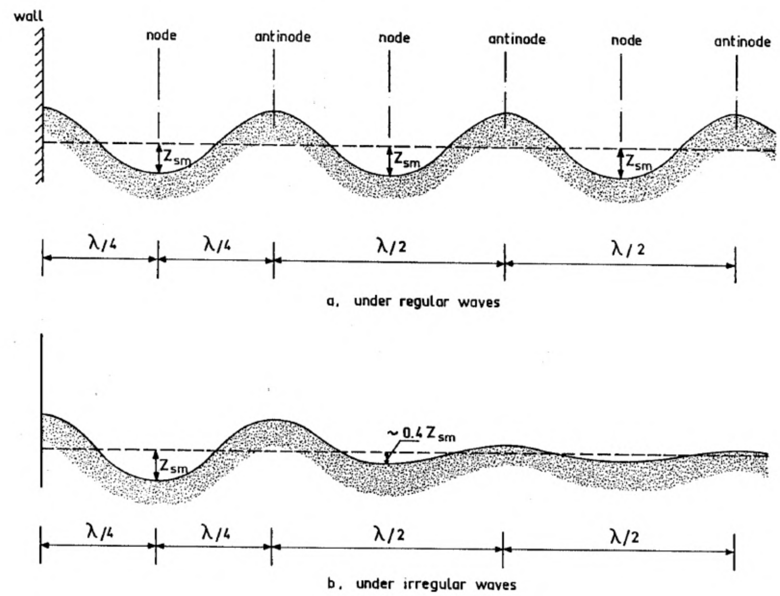

Figure 2.5: Scour profile under regular and irregular waves. (With λ as wavelength) Xie (1981)

maximum amplitude and because of that maximum scour. Thus, when the reflection coefficient or reflection are decreased, scour will also decrease. The following parameters have an influence on the reflection coefficient and thus on the scour:

- The permeability of the structure: A higher permeability of the structure leads to a lower reflection coefficient.
- The smoothness of the slope: A higher smoothness results in a higher reflection coefficient.
- The steepness of the slope of the structure: A steeper slope of the structure is accompanied by a higher reflection coefficient.
- The steepness of the incoming wave can be expressed in different dimensionless numbers such as, the breaking parameter or the fictitious wave steepness. A steeper wave causes a lower reflection coefficient.

The other mentioned mechanism is the downrush flow of the wave along the structure. When the seabed is not protected this can lead to scour close to the structure. The same parameters mentioned for the reflection coefficient are also important here. However, this mechanism is only relevant close to the structure while the standing wave pattern can have an impact on the structure while a few wavelengths away. A toe protection is often the solution to counter the downrush flow since the bed closest to the structure is well protected with a toe.

The toe structure is often used as scour protection. In many cases an additional scour protection, in form of a bed protection, is installed to bring scour further away from the structure. This avoids sliding of the embankment slope in to the scour hole. This bed protection can be an extension of the toe using smaller stones, which is usually more economic. This theses researches both the effect of a toe and a toe with an additional bed protection, fig. 2.6.

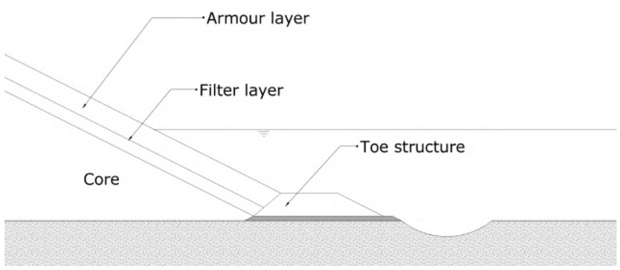

(a) Sloped embankment with only a toe structure.

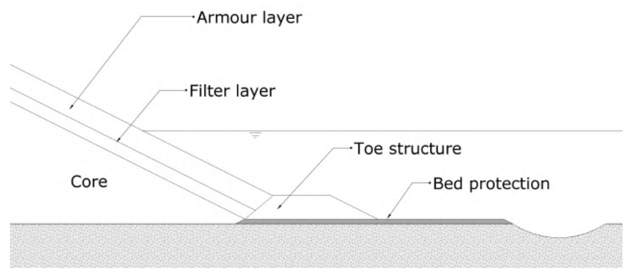

(b) Sloped embankment with an additional bed protection.

Figure 2.6: Comparison scour location with only a toe structure and with an additional bed protection.

2.3.1 Research done by Sumer and Fredsøe.

Sumer and Fredsøe (2000) focused on the relation between scour and the protection against scour in their research. Sumer and Fredsøe performed physical tests in a wave flume with a length of $28m$. The height and the width of the flume where $0.6m$ and $0.8m$ respectively. Multiple breakwater configurations were tested, as well as one test with a vertical wall for reference purposes. A total of 37 tests were performed with varying wave conditions. These were two breakwater slopes and different or no scour protections mechanisms. Most test cases were with regular waves, a few tests have been performed with irregular waves. The tests were executed up until an equilibrium bed profile was reached. In fig. 2.7 the equilibrium bed profile of three different tests with irregular waves is shown.

The results shown in fig. 2.7 are from tests without a scour protection. The pattern of the bed profile can, just as in fig. 2.5, be related to the wavelength. The relation is less strong when compared to a vertical wall or regular waves. It can also be seen that the wavelength has an influence on the location of the scour and thus the stability of the sloped embankment. To protect against scour close to the structure, large stones were placed as toe structure in other tests. The thickness and the length of the scour protection was varied to research the correlation between the two variables. The results of these tests together with all the other test variations are summarised in the list of conclusions below, Sumer and Fredsøe (2000).

- The 2D scour pattern in front of a rubble mound structure emerges alternating in scour and deposition, with a relation between the scour pattern and the wavelength.
- The scour at a rubble mound breakwater is smaller than at a vertical-wall breakwater.
- The scour depth decreases with a more gentle slope of the rubble mound structure.
- The scour depth is lower for irregular waves compared to regular waves.
- If the length of the scour protection (protection apron) is equal to the width of the scour hole, the bed is completely protected against scour.
- The protection apron slumps down into the scour hole, creating a protective slope. An increasing thickness (layers of stone) of the protection apron increases the effectiveness of this slope. However, after a certain number of layers increasing the thickness is not effective anymore.

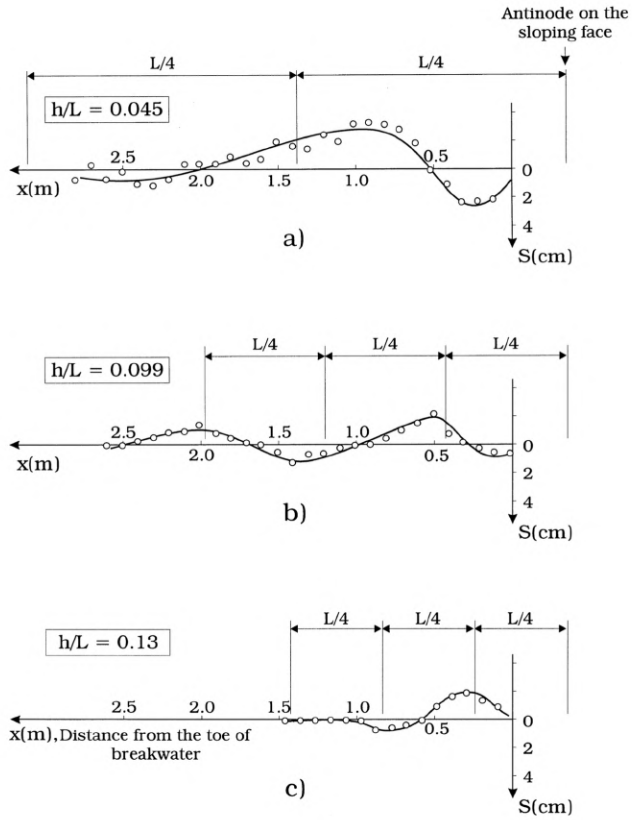

Figure 2.7: Equilibrium bed profile for irregular waves. Sumer and Fredsøe (2000)

2.3.2 Research done by den Bieman

A recent research by den Bieman et al. (2019) performed physical model tests on toe scour at a sandy bed in front of rubble mound structures. In these tests, scour was measured underneath and in front the toe of an impermeable rubble mounted structure with a maximum test duration of 3000 waves. In the research of Den Bieman a linear relation was found between the number of waves and the amount of scour, this can be seen in fig. 2.8. This indicates that there is a possibility that much more than 3000 waves are needed to find an equilibrium for the scour depth. The research also shows that the toe structure sinks slowly, but linearly, into the seabed. This is due to the fact that a filter layer between the toe structure and the sand has not been used.

Although there are some differences in the research of den Bieman et al. (2019) and this theses it can still be used reference material. The Scheldegoot, which is the wave flume used by den Bieman, is fairly similar in size to the wave flume used at the TU Delft. The Scheldegoot has a length of $55m$, a width of $1.0m$ and a height of $1.2m$. This means that both test series can be compared without having to consider scaling issues. Furthermore, van Bieman recommends that toe configuration and structure slope should be varied. Van Bieman also writes that physical model tests with artificial sand could give more insight. In a discussion however, den Bieman did state that this would mainly be useful when it could be compared to large scale model tests.

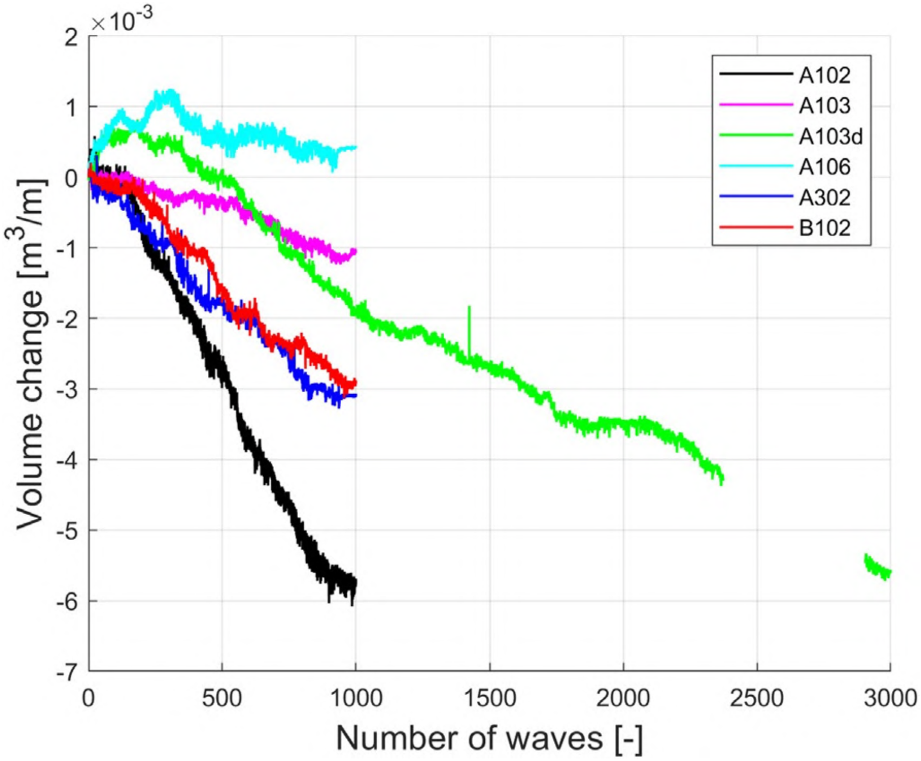

Figure 2.8: Scour compared to number of waves. den Bieman et al. (2019)

2.4 Scaling laws

In this research the physical scale model does not resemble a prototype. The tests are process based, meaning that the general process of scour in front of a sloped embankments is investigated and not the scour in front of a specific structure. However, this does not imply that scale effects are not in place. The test results will be used for large scale sloped embankment design, thus it is also required that they are valid for full scale prototypes. Since the forces in water are not linear, they can not all be correctly scaled. If for instance Froude-scaling - meaning that the Froude number stays the same - is used, the inertia forces and the gravitational forces are correctly scaled. Other forces, such as viscous forces, are however incorrectly scaled, which can cause large scale effects if theses forces would be dominant.

The scaling problems in physical modelling were elaborately described firstly by Hughes (1993) and later by Frostick et al. (2011). Three different similarities are considered for the scale model: the geometric, kinematic and dynamic similarities.

- Geometric similarity implies that the ratio of any length dimension is scaled corresponding to the other length dimensions. So, there are no changes in the shape of the scale model.
- Kinematic similarity means that the streamline patterns, velocity and acceleration are all related in a constant ratio. This is also referred to as 'similarity of motion' by Papadopoulos (2012).
- Dynamic similarity only exists when forces on corresponding points of the prototype and scale model are similar. Forces which are considered for fluid mechanics are: inertial, gravitational, viscous, surface tension, pressure and elastic forces.

2.4.1 Dynamic similarity

A limitation of the dynamic similarity is that not all forces can be scaled simultaneously. The forces are represented in the different scaling laws of which Froude-scaling was already mentioned. Dependent on the importance of other individual forces, other various scaling numbers have been introduced: Reynolds, Weber, Mach, Cauchy, Richardson, Euler and Strouhal (Frostick et al. (2011)). The important scaling laws for this research are:

- Froude: $Fr = \frac{inertial force}{gravity force} = \frac{u}{\sqrt{gL}}$
- Reynolds: $Re = \frac{inertial force}{viscous force} = \frac{uL}{\nu}$
- Weber: $We = \frac{inertial force}{surface tension force} = \frac{\rho_w u^2 L}{\sigma}$
- Cauchy: $Ca = \frac{inertial force}{elastic force} = \frac{\rho_w u^2}{E}$

The inertial force is considered important in all the scaling laws, however the other forces are only present in one scaling law. For waves the surface tension, inertia and gravity forces are relevant while viscous forces are important to define the force of the water on the sand or rock particles. According to Hughes (1993) only one scaling law can be used when the same fluid is used for the prototype and the scale model, which is usually the case. Thus, this implies that the most relevant force and scale law has to be selected. As, other forces will be scaled incorrectly, inevitably scale effects will occur.

2.4.2 Froude scaling

The wave field is mostly influenced by gravity en inertia, so Froude is almost always used as modelling law for applications with waves and a sloped embankment. When the Froude number is used the scaling of bottom friction is ignored as well as the scaling of viscous forces and surface tension. Bottom friction is negligible since waves have to propagate along large distances before it has a considerable effect. This is not the case for testing scour due to waves at sloped embankments. The surface tension could cause scaling problems if the waves in the model are too small. To avoid this the wavelengths have to be larger than $2cm$ and the wave period larger than $0.35s$, Frostick et al. (2011). If this criteria is met the Weber number can be neglected. Another problem at sloped embankments can be the intake of air in the water while waves are breaking. This is only a problem when the scale is too small, then the Weber and Cauchy numbers are of importance. In practice this leads to scaling problems for the stability of the armour layer. However, in this case the stability is not considered, and therefore this will not cause noticeable scale effects.

Similarly, the Reynolds number also does not have to be exactly the same for the prototype as for the scale model as long as both are in the same range. However, the Reynolds number is more important to consider compared to the Cauchy or Weber number. For prototype scale breakwaters the flow is turbulent and the Reynolds number is large. If the flow is turbulent in the scale model, Froude scaling can be used and Reynolds can be neglected. However, since for a scale model the armour units, bed protection and toe structure will all be scaled down it is possible that the flow inside the structure becomes laminar at some locations. In this case Frostick et al. (2011) proposes two criteria, which have to be met for Froude scaling:

- The Reynolds number in the construction, eq. (2.10), has to be larger than 3000.
- Diameters have to be larger than $3mm - 5mm$ in the armour filter layer of the scale model.

$$Re_d = \frac{\sqrt{gH_s d}}{\nu} \tag{2.10}$$

Thus, the criteria for a scale model of a sloped embankment are dependent on multiple scale numbers and forces. As long as the scale model is not too small these criteria are easily met. However, the scaling of sediment is more challenging since sand is difficult to scale down.

2.4.3 Sediment scaling

The seabed in front of a sloped embankment often consists of sand. Sand has a grain size between $0.062mm$ and $2mm$. If this is scaled down it could get problematic if the scaled down to smaller than $0.062mm$ the sediment has a more cohesive character, which influences the amount of scour. For larger scale factors, wide graded sand or small sand in the prototype bed, sand can not be scaled properly. Therefore, the geometric similarity can not be met for a physical model of scour in front of a sloped embankment.

When Froude scaling is used, the inertia forces and the gravitational forces are correctly scaled. However, this causes some problems for the viscous forces, which implies that the suspended sediment transport is not completely correct. This follows from the fact that the Shields parameter and the fall velocity can not be scaled perfectly. Besides that the grain size of the sand will be relatively large in the scale model test. The sand can, however, not be smaller since this would induce cohesive behaviour of the sediment. The initiation of motion for sand is not significantly affected by these scale effects. However, it could lead to a distorted time scale since the bigger sand particles have a smaller velocity. This means that it takes longer for an equilibrium or a certain scour depth to be reached.

An optional modelling method to reduce some of these scale effects and still comply with the scaling laws could be to use artificial sediment (light weight material). A lighter material could be used for sand so that the grain size can be larger. Because of this both the Froude number and the Reynolds number can be scaled correctly. However, this does introduce some new scale effects which can significantly influence the behaviour of the model. These scale effects follow from the incorrect scaling of relative density, larger grain size and higher porosity of the sand bed. When the results of a scale model test could be compared to a larger scale model or prototype this might be useful. In most cases it still causes significant scale effects while not providing a big advantage and is often not used.

For this research conventional sand was used to perform the test. Based on literature and expert judgement it is concluded that artificial sand adds multiple uncertainties. Besides that, it is hard to come by and only available in one single grain size in the fluid dynamics laboratory of Civil Engineering. In order to research issues due to the earlier discussed distorted time scale, an extremely long duration test is performed.

2.5 Parameters of influence

From the former sections of this chapter it can be concluded that a large number of parameters have an influence on scour in front of a sloped embankment. In the list below an overview of the needed parameters is given for this research. Some of these dimensions are clarified in fig. 2.9

- **Wave conditions** Height (H), length (L) and period (T).
- **Test duration**, number of waves (N) and duration (D).
- **Water depth** (h).
- **Embankment dimensions**, steepness of slope (α), permeability (P) and the grain size ($d_{n50,armour}$) of armour layer.
- **Toe dimensions**, width (W_t), thickness (t_{toe}) and, the density (ρ_s) the grain size ($d_{n50,toe}$).
- **Bed protection dimensions**, width (W_{bp}), thickness (t_{bp}, the density (ρ_s) and grain size ($d_{n50,bp}$).
- **Sand properties**, the density (ρ_s) and the grain size ($d_{n50,sand}$).

From the literature study it can be concluded that besides the bed protection, many more parameters have an important influence. For this research, the wave conditions, permeability and the hydraulic conditions were also varied. For the hydraulic conditions an offshore wave steepness between 1$ and 4% is used This corresponds to earlier research done by Sumer and Fredsøe (2000) and den Bieman et al. (2019). Although flatter waves were tested by den Bieman, they are not included in this research. For this research only waves which comply with linear wave theory are used. The exact used conditions in this research are described in chapter 4.

Furthermore, from earlier studies, it can also be concluded that a long test duration is needed. since den Bieman et al. (2019), performed a test with 3000 waves without reaching an equilibrium. In this research at least 15000 waves are used every test. The number of waves for each test can also be found in chapter 4. Finally for the permeability, a fully impermeable slope and a permeable slope with $P \approx 0.4$ is used. This corresponds respectively to for instance a dike and a breakwater.

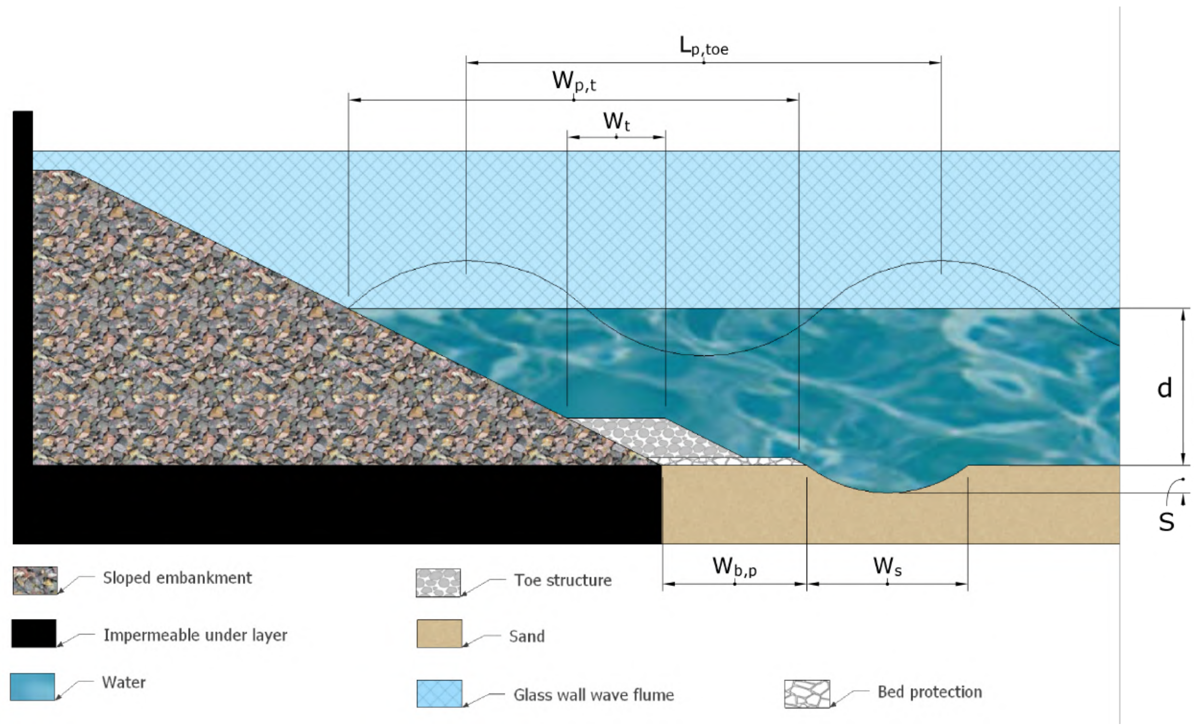

Figure 2.9: Parameters sloped embankment model.

Chapter 3

Experiment set-up

In this chapter the experiment set-up is reviewed. First of all, a short overview is given of the essential elements for the experiments. This follows from the literature study done in chapter 2. Secondly in section 3.1, the available wave flume for this research is discussed, since this limits the dimensions of the physical model. This physical model is shown in section 3.2 and the chosen dimensions are elaborated on. The rubble mound structure and the bed protection are explained in respectively section 3.2.1 and section 3.2.2. In appendices A and B the toe stability, armour layer and the sand properties are discussed to support the final physical model design. Finally, the used measurement devices are described in section 3.3.

In section 2.5 all of the parameters, which could both vary in the designs of sloped embankments and influence scour in front of the structure, are listed. However, it is not possible to test the influence of every parameter due to limited time and resources. Besides, not every parameter has the same influence and former research already describes the influence of a large part of these parameters. Thus, the parameters, which are most important for scour and not yet researched, will be tested in this research. However, to make a realistic scale model all parameters are considered in the design of the experiment set-up.

The main parameter, which is researched in this thesis, is the bed protection. Besides that, it followed from the literature study that the permeability and the hydraulic conditions have a large influence on scour. This is why these two parameters are also varied in this study. In chapter 4 the exact parameters used in the tests are discussed. For the experiment set-up it is important that these parameters can be easily varied in between tests. From this a few aspects are taken to consider during the design of the experiment set-up:

- A large sandpit is needed, which can support scour patterns, for different wave conditions and multiple bed protection configurations.
- The physical model (containing sloped embankment, toe structure and bed protection) has to be easily removed or placed.
- The experiment set-up has to be designed in such a way that the hydraulic conditions can vary without having to change the physical model.

3.1 Wave flume

For this experiment the available wave flume is located at the fluid dynamics laboratory of Civil Engineering at the Technical University of Delft. The dimensions of the flume are summarised in the list below. The working height is just above $1.0m$ so that the maximum construction height is also $1.0m$. When using the wave generator the water depth in the flume can be varied from $0.3m$ up until $0.9m$. However, limiting the water depth also limits the wave height which can be produced in the flume. Besides that, when maximising the water depth the waves role over the flume if they are to large. The maximum capacity of the wave generator are irregular waves with a significant wave height of $0.3m$ with a peak period of $2.0s$ in a water depth of $0.7m$. In the next section more aspects will be discussed, which need to be considered, for the used hydraulic conditions. The waves which are generated by a piston type wave generator actively absorb the reflected waves.

- Flume width: $0.79m$
- Flume height: $1.0m$
- Flume length: $42.5m$
- Water depth: $0.3m$ – $0.9m$
- Maximum theoretical significant wave height: $0.3m$

The theoretical values of the wave parameters in the flume are however not practical. If the wave period is longer or the depth shallower, the waves cannot be as large as the theoretical value. In this research the offshore water depth is $0.6m$ and the maximum wave period $2.5s$. The maximum feasible significant wave height for these conditions is $0.18m$.

3.2 Physical model set-up

The scale of the physical model is constrained by the dimensions of the flume. The height of the flume is the most important constraint. The needed height consists of the thickness of the sandpit, the local water depth and the wave run-up. The value of these parameters and their relation to the wave height are listed below. In the next section it is explained how these parameters are combined.

- **Thickness of the sandpit $<$ wave height**. In literature, such as Dont and Laborie (2007), it is often stated that the maximum scour depth is equal the wave height in close to the structure. Specifically the maximum wave height or the significant wave height which can be supported by the water depth just in front of the structure. This is however for vertical or steep walls, thus it is likely less in this research. In this research, the thickness of the sandpit is $0.215m$.
- **Water depth above the sandpit $\approx$ 2 x wave height**. The water depth is also related to the maximum wave height, since it has to be able to support the waves coming towards the structure. The maximum wave height which can be supported is $0.35-0.8$ times the water depth Simm et al. (1996). However, in wave flumes this is for relatively flat slopes around 0.5 times the water depth, Nelson (1994). Thus, the water depth can be described as two times the wave height. In this research a water depth above the sandpit of $0.385m$ is used.
- **Wave run-up $\approx$ 2 x significant wave height**. On a rubble mound structure the maximum wave run-up is equal to two times the significant wave height, Dont and Laborie (2007). For smooth and permeable structures, the run is however more ($3*H_s$ to $3.5*H_s$). The available height for wave run up in this research is equal to $0.4m$.

The scour can be equal to the wave height and the maximum possible wave height is approximately half the water depth. Thus, the water depth has to be two times the sandpit thickness. For the wave height however, multiple formulations are possible. The wave height can be expressed in significant wave height (H_s), highest 1% waves, maximum wave height and much more. The H_s is often used in calculations, which is also the case for the the wave run-up. For the maximum wave height which can be supported by the water depth, the maximum wave height is however needed. The wave heights are Rayleigh distributed, from which follows that the maximum wave height (1 in 3000 waves) is equal to $2*H_s$, Mangor (2020). The highest 1% of the waves is in turn equal to $1.5*H_s$.

Combining this knowledge and the wave flume parameters the decision is made to aim for a sand bed with a thickness of $0.2m$ and a water depth close to the structure of $0.4m$. Besides that, $0.4m$ is available for the run-up of waves. The used dimensions can be seen in fig. 3.1. With the choice of these dimensions, not all the waves which can be generated in the flume can be supported by the water depth. This results in some breaking waves on the foreshore when a H_s larger than $0.1m$ is used. Besides that, the maximum run-up for smooth structures could be higher than $0.4m$ if a H_s larger than $0.12m$ is used. The following two assumptions are made for a wave spectrum with a large significant wave height:

- The maximum run-up is equal to $2 * H_s$ for rubble mound structures, which can support all possible wave heights in the flume. For smooth and permeable structures, the run is however more ($3 * H_s$ to $3.5 * H_s$). As long as overflow not allowed and run-up is limited, large wave heights can be used. A crest wall can be constructed to prevent overflow.
- The maximum wave height cannot be supported by the water depth for a H_s larger than $0.1m$. Higher significant wave heights can be used, as long as most of the waves can be supported. The Rayleigh distribution is used to determine how much waves will break on the foreshore.

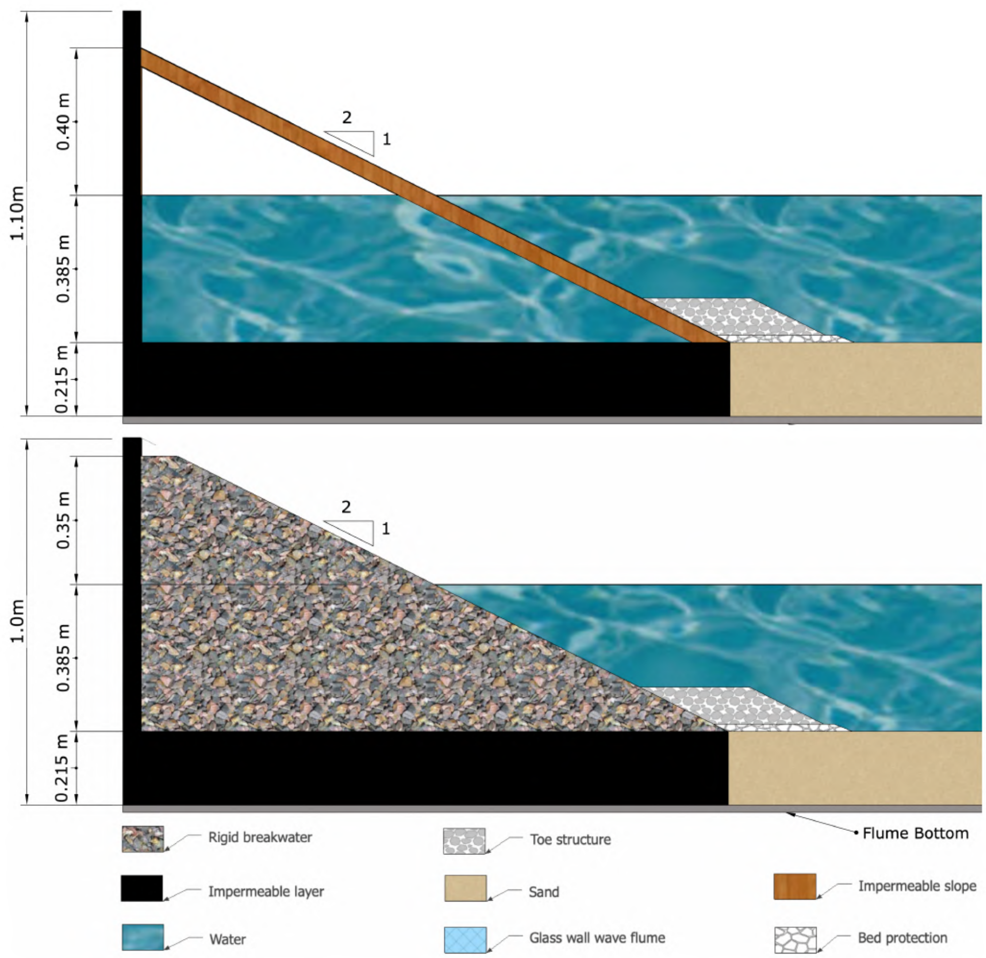

Figure 3.1: Test set-up vertical dimensions. *Either permeable slope or rigid breakwater is used.*

Since the sandpit in the wave flume is $0.2m$ higher than the bottom of the flume, a ramp has to be constructed. This serves as foreshore with a gentle slope. The slope of the foreshore is 1/30, just as in the research of den Bieman et al. (2019). A horizontal transition plane is placed between the slope and the sandpit. Both these section have a length of $6m$ and are made out of wood. The total length of the sandpit and the sloped embankment are just above $10m$. The length is just more than two times the local wavelength so that a clear bottom pattern can form. In fig. 3.2 the experiment set-up is shown with focus on the dimensions in the cross shore direction.

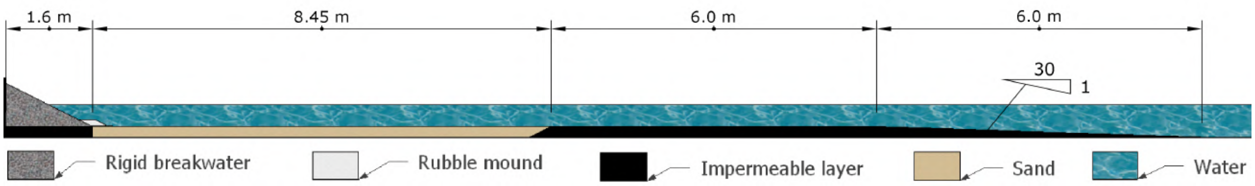

Figure 3.2: Cross section wave flume. (Flume extends approximately 20m in offshore direction.)

In fig. 3.2 the deep water part of the flume is not shown since no structures are built there. The breakwater can be seen on the left side of the flume and will be discussed in more detail in the next section. The slope of this breakwater is a 1 : 2 slope. This is slope is also used in existing rubble mound structures and also used by den Bieman et al. (2019). These two aspects make certain that it is comparable to existing research and realistic for future designs. For tests with an impermeable structure this breakwater is simply replaced with a wooden plank.

3.2.1 Structure

Different configurations for the rubble mound structure and the impermeable slope were used in the experiments. Thus, the permeability of the structure was varied and the amount of bed protection. All the different configurations are listed in table 3.1.

Description + Test number	sketch
Impermeable structure without bed protection. (Test A.1 & A.2)	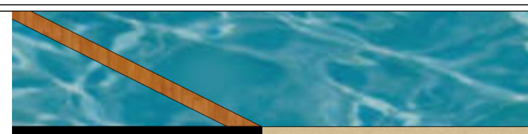
Impermeable structure with a toe structure which is supported by a filter layer. (Test A.3 & A.5)	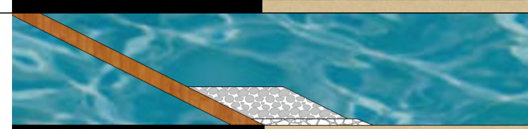
Impermeable structure with a toe structure which is supported by a filter layer. This filter layer extends seawards to function as a longer bed protection. (Test A.4)	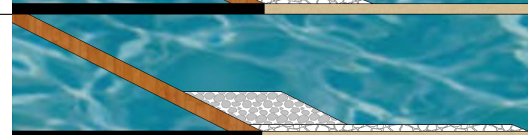
Permeable structure without bed protection. (Test B.1)	
Permeable structure with a toe structure which is supported by a filter layer. (Test B.2, B.3 & B.5)	
Permeable structure with a toe structure which is supported by a filter layer. This filter layer extends seawards to function as a longer bed protection. (Test B.4)	

Table 3.1: Structure configurations in experiment.

In fig. 3.3 one of the physical model configurations is shown. For all tests the same materials were used for the toe structure, sand and bed protection. The tests were performed using either a wooden plank functioning as impermeable structure or a breakwater functioning as permeable structure. The breakwater and toe structure have a d_{n50} of $38mm$, the bed protection has a d_{n50} of $7.8mm$ and the sand pit has a d_{n50} of $0.26mm$. The choices and grading curves for the materials of the breakwater, bed protection and sand layer are discussed in respectively appendix A, section 3.2.2 and appendix B. Typical parameters of the materials are given in the table below, table 3.2.

Material	d_{n15} $[mm]$	d_{n50} $[mm]$	d_{n85} $[mm]$	d_{n85}/d_{n15} $[-]$	ρ_s $[kg/m^3]$
Breakwater and toe structure	29.8	38.0	44.1	1.48	2.557
Bottom protection	4.91	7.82	11.47	2.34	3035
Sand	0.21	0.26	0.32	1.52	2650

Table 3.2: Material properties. *For sand the parameters d_{15}, d_{50} and d_{85} are used.*

The rock material of the main structure has been glued together to prevent long rebuilding times in between tests. In appendix C it is discussed how this breakwater was built. The toe structure consists of loose gravel material so that a reshape of the material can occur. The toe structure is rebuilt manually after each test with exactly the same stones. To keep it as similar as possible between tests, a ruler and a spirit level were used to built the toe. To a large extent the structure is identical between tests, however small differences were present. The thickness and width of the toe are chosen at respectively $2d_{n50}$ and $5d_{n50}$, see also fig. 3.3.

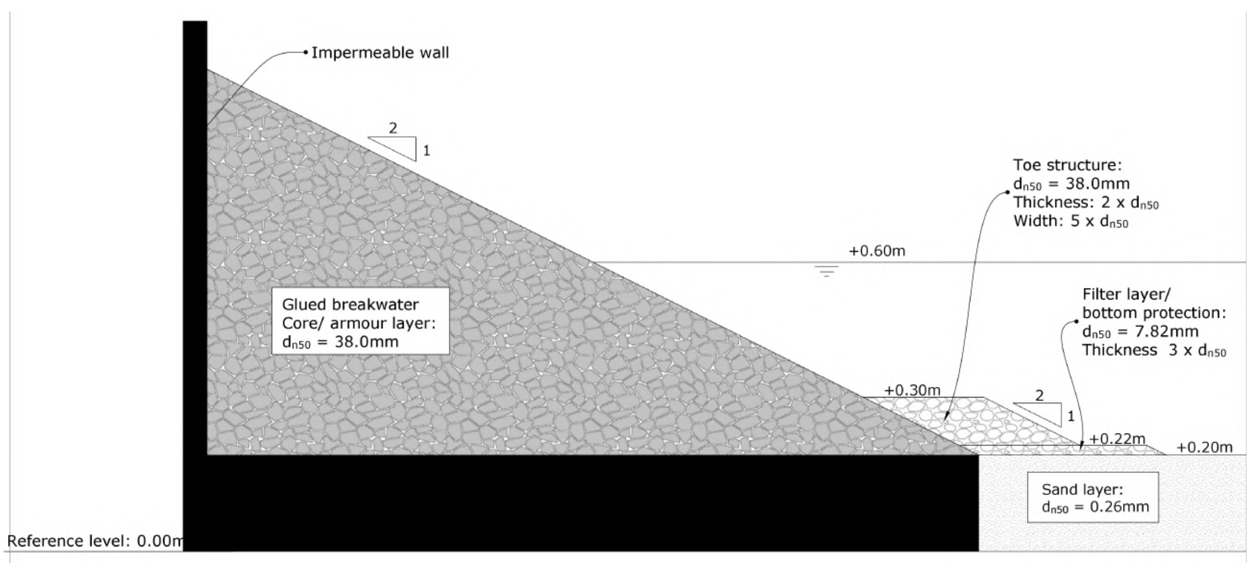

Figure 3.3: Physical model with breakwater including used grain sizes. *For impermeable slope see appendix F.*

3.2.2 Bed protection

The bed protection lies upon the sand pit and functions as filter layer between the sandpit and the toe structure. The sand layer is constructed using loose sand which is flattened but not compacted. Because the same material is used for the filter layer and the bed protection, multiple requirements have to be met by this material:

- The bed protection has to be stable under the incoming waves, only initial movement is allowed, Shields (1936).
- The bed protection has to satisfy the criteria for internal filter stability and stability between the filter layer and the toe structure. These criteria are described by Schiereck and Verhagen (2012).
- Winnowing of sand trough the bed protection must be minimised, fig. D.2.

To satisfy all these criteria, basalt split is used with a d_{n50} of $7.82mm$, table 3.2. Furthermore, the thickness of the bed protection is $3d_{n50}$. The criteria and the chosen dimensions are further discussed in appendix D. The bed protection is placed in a similar manner as the toe structure, using a ruler and a spirit level. Multiple sections with different colours were used so that it is more easy to see movement of the protection layer.

3.3 Measurement devices

For measuring the needed parameters different instruments were available. In the list below, it is stated which parameters can be measured, by which instrument. To follow the same procedure a test procedure is used. This procedure can be found in appendix E.

- **Wave gauges** were used to measure the wave conditions in the wave flume. Two sets of three wave gauges were used so that the waves on top of the fixed foreshore and waves in front of the wave paddle can be measured, fig. 3.4. Because three wave gauges were used at both locations the reflection of the waves from the structure can be calculated. The wave gauges produce a water elevation signal. To decompose this signal the Matrix decomposition method, described in Msc-thesis of Henk Jan Bakkenes (June 2002), is used. The Matlab script for this method written by Bakkenes and H. Klaasman generates as output the typical wave parameters.
- **Laser distant sensors** were used to measure the bed level. The distance between the laser sensors and the bed is measured before and after each tests. A fixed reference point is used to calibrate the different measurements with each other. When the distance between the sensor and the bed before and after the test are compared, the difference is the erosion or accretion. For each tests 8 profiles are measured before and after the tests. During the test 2 profiles are measured at increasing time intervals. The laser sensors measure 10000 points per meter, or 10 points per millimeter.
- **Cameras** were used to measure the scour in side view during the test. This so, that a trend in time can be observed of the scour hole. The pixels in the pictures have a certain pixel density and can be expressed as pixels per meter. When the location of the sand bed is related to a certain pixel, the distance between that location and any other point in the picture can be determined. When a fixed point in the picture and the location of maximum scour are used, the maximum scour depth can be extracted.
- **Electromagnetic Flow Meter (EMS)** was used to measure the mean flow velocity due to the waves. The EMS is used in a few tests to measure the flow close ($\approx 10cm$) to the original sand bed. This is an oscillating flow, but the mean value of this flow velocity is used. This is used to verify certain observations in the test series with measurements.

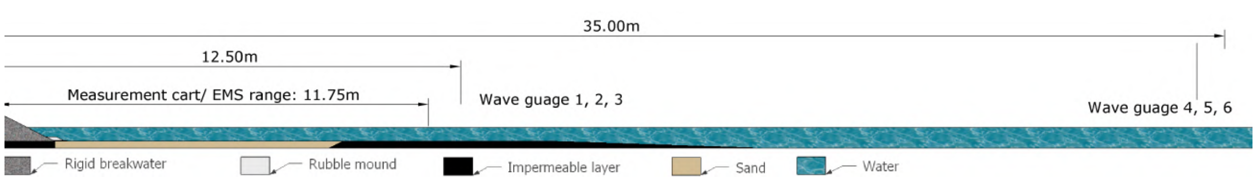

Figure 3.4: Location instruments

The laser distant sensors are mounted on a measurement cart, fig. 3.5. This cart can move along rails, which are attached to the wave flume. An impulse wheel is used to measure the location of the cart and when moved sent a signal to the lasers. When the laser sensor and the impulse wheel are combined every laser measurement is coupled to a cross shore location. The laser sensors can also be moved along the width of the flume by using a slider fitted with a scale. This is however not coupled to a location, thus it has to be written down manually. Besides that, the laser sensors are moved in and out of the water (up and down) by hand. The exact location of the measurement devises is also determined with a scale.

Figure 3.5: Measurement cart

The accuracy of the scour measurements is therefore mainly determined by the inaccuracies of the manual displacements of the instruments. In the processing of the raw data it is important to calibrate everything using fixed points in the test set-up. This can eliminate any potential measurement errors. However, the calibration points have an inaccuracy of a few millimetres. Therefore, the accuracy of the scour measurements executed with laser sensors is equal to a few (2-3) millimetres.

For the measurements with the cameras measurement errors occur in a comparable order size. Even though the cameras and the calibration points are fixed. The processing of the data is done manually by clicking on the needed locations in the picture. This location can be either the calibration point or the bed level. It is however difficult to manually choose the exact pixel, especially since these pictures are often made while testing. Thus, the turbidity of the water and the inability to click exactly at the wanted pixel result in a measurement error of a few (2-3) millimetres.

Chapter 4

Test program

The focus of this research is the influence of the bed protection on the scour in front of a sloped embankment. Two series of tests are done to research this, with either the breakwater as described in appendix C or a wooden plank functioning as impermeable structure. In these test series, the length of the bed protection and the hydraulic conditions have been varied. Initially, only a permeable structure would be tested, since the knowledge gap is larger for permeable structures. For both practical reasons and the importance of permeability for scour, it was decided to also do tests on a impermeable structure. Furthermore, this gives more opportunities to relate this research to previous works.

4.1 Hydraulic conditions

The test are all conducted in a offshore water depth of $0.6m$. The sand layer has a thickness of $0.215m$ and the water depth at the location of the toe is equal to $0.385m$. For the waves an irregular wave field is used, which mostly constant for the different tests. The initial wave field has offshore H_s of $0.14m$ and a T_p of $1.6s$. The Jonswap spectrum has been used to represent these irregular waves. This wave condition was chosen in such a way that clearly visible scour is expected. Besides that, room for bigger or smaller waves is available in case of respectively to much or minimum scour. Only a small amount of scour was visible after the first test, so longer waves are used in most of the other tests. Since, more scour is expected for longer waves and a better visible scour pattern. In each test series one variation is used to investigate the influence of the hydraulic condition.

4.2 Length bed protection

To study the influence of the bed protection on the scour three layouts are used. No bed protection, only a toe structure and a toe structure combined with a longer bed protection, table 3.1. The longer bed protection will have a length of $1.0m$ including toe structure. The total bed protection length, including the submerged part of the breakwater, is in this case equal to $1.8m$. The combined bed protection length ($W_{p,t}$ see fig. 2.9) is related to the scour pattern. The total bed protection is equal to 3/8 wavelength for a period of $2.5s$ and 5/8 wavelength for a wave period of $1.6s$. It is expected that this will respectively be just before an anti-node and a node, fig. 2.7. For both wavelengths, the combined length covers the whole scour hole, closest to the structure, as shown in fig. 2.5.

Both test series have three test with the same hydraulic conditions and varying bed protections. In this way the influence can be determined with minimal interference of other parameters. For the toe structure the same stones are used for every test. For the bed protection this is not possible, thus the same amount of stones are used in between tests. Each test series also contains a repetition test to determine the precision of the experiment.

4.3 Test schedule

The two test series consists of a total of ten tests. In the list below the important parameters are described. This is followed by table 4.1 and table 4.2 containing respectively test series A and B.

- H_s: Significant wave height at the toe location. The local wave height differed with the input of the wave maker, thus the input value is shown between brackets.
- T_p: Peak period.
- $W_{b,p}$: Length bed protection, including toe structure.
- $W_{b,t}/L$: Length bed protection, from intersection slope and waterline up to end bed protection, related to local wavelength.
- D: Duration of the test (model scale).
- N: Number of waves.
- $s_{o,p}$: Offshore wave steepness, calculated with input values.
- K_R: Reflection coefficient waves at the onshore measurement location.

Test	$H_s[cm]$	$T_p[s]$	$W_{b,p}[m]$	$\frac{W_{b,t}}{L}[-]$	$D[hour]$	$N[-]$	$s_{o,p}[-]$	$K_R[-]$
A.1	12.1 *(14)*	1.6	0	0	10	22500	3.5	0.63
A.2	13.5 *(14)*	2.5	0	0	66	95000	1.4	0.81
A.3	13.4 *(14)*	2.5	0.25	1/4	16	23000	1.4	0.78
A.4	13.5 *(14)*	2.5	1.0	3/8	32	46000	1.4	0.77
A.5	12.2 *(14)*	1.6	0.25	3/8	128	288000	3.5	0.61

Table 4.1: Test series A: Tests for an impermeable structure with a 1 in 2 slope. *Wave height between brackets is the target value, measured H_s is incoming wave height at wave gauge location 1,2,3.*

Test	$H_s[cm]$	$T_p[s]$	$W_{b,p}[m]$	$\frac{W_{b,t}}{L}[-]$	$D[hour]$	$N[-]$	$s_{o,p}[-]$	$K_R[-]$
B.1	13.9 *(14)*	2.5	0	0	32	46000	1.4	0.43
B.2	13.9 *(14)*	2.5	0.25	1/4	16	23000	1.4	0.40
B.3	17.1 *(18)*	2.5	0.25	1/4	22	32000	1.7	0.43
B.4	14.0 *(14)*	2.5	1.0	3/8	8	11500	1.4	0.42
B.5	14.0 *(14)*	2.5	0.25	1/4	8	11500	1.4	0.41

Table 4.2: Test series A: Tests for an impermeable structure with a 1 in 2 slope. *Wave height between brackets is the target value, measured H_s is incoming wave height at wave gauge location 1,2,3.*

An overview of additional wave parameters ($T_{m-1,0}, T_{m0,2}, H_{max}$) and the offshore wave conditions are presented in appendix G. Furthermore, the bed profile is flattened after each test to start each test with the same conditions. Photographs of the bed level close to the structure (first three meters) are taken every hour to determine the development in time of the scour depth. Although, the tests have a different duration, laser measurements are done at certain time intervals to be better able to compare tests. Namely after 0.5, 1, 2, 4, ,8, 16, 32, 64 and 128 hours, depending on the test duration.

Chapter 5

Test results and observations

In this chapter the results of the tests are presented. First of all, it is discussed which results are available and how these are shown. Secondly, the scour measurements results of test series A, with the impermeable structure, are presented. Each graph is supported with a picture in side view of the bed profile close to the structure. After that, the scour measurements results of test series B, with the permeable structure, are presented in a similar way. Finally, additional scour measurements performed with a camera are discussed.

In this research, the laser sensors provide the most important measurement results. This since the whole sand bed can be measured in detail. Besides that, the measurements at different time intervals provide insight in the development of scour over time. The photo measurements are used to support the findings with the laser measurements, but since they do not cover the whole sand bed they can not be used to sketch a bottom profile. However, the photo measurements are used to characterise the development of the maximum scour depth close to the structure.

5.1 Laser measurements

In fig. 5.1 a schematic view of the flume is shown, which is used to present the results in sections 5.1.1 and 5.1.2. The figure shows the initial bed profile, bed protection, toe structure and sloped embankment. It also shows the waterline, surface elevation and the bed profile after a test. Finally, the distance to the structure (point where the water line crosses the slope) related to the peak wavelength is plotted. Since, as discussed in chapter 2, the scour pattern relates to the local wavelength. Further figures are focused on the bed profile, while the same general schematic view is used.

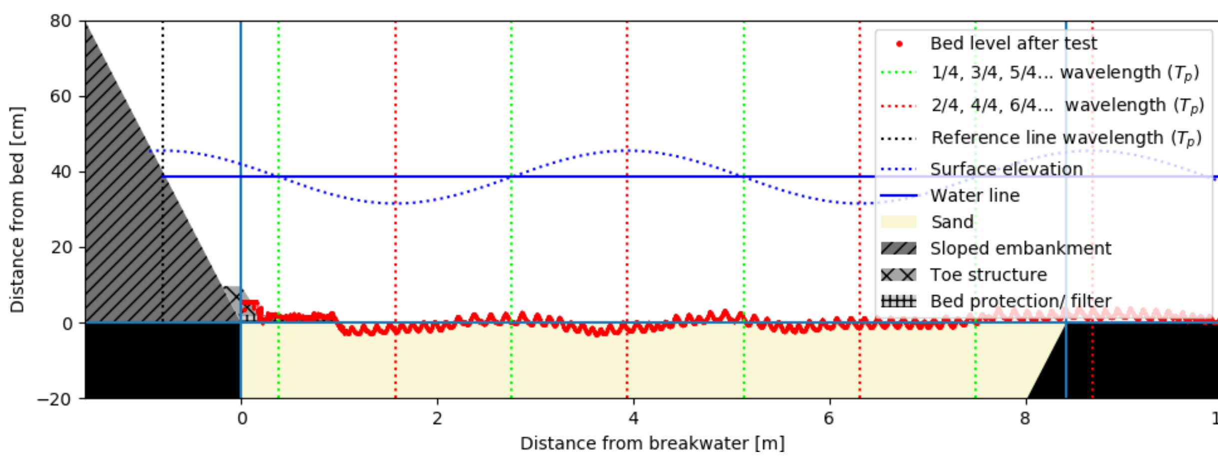

Figure 5.1: Reference figure, schematic view of results laser measurements.

During testing, after a few minutes, small sand dunes (ripples) originate due to the waves. These ripples can be seen in the laser measurements, fig. 5.2, and also clearly visible on the pictures taken during the tests, figs. 5.3a and 5.4a. The ripples stay small (height $\approx 2cm$, length $\approx 10cm$) during testing, this research focuses on larger bed patterns and therefore ripples are not considered. Another reason to not consider these ripples is the inability to scale them from small scale to large scale, O'Donoghue et al. (2006). The ripples are filtered out by using a moving average with the length of a single sand dune. Besides that, the average of all the different measured cross section is used for the results and analysis. In fig. 5.2, it is shown how the raw scour data, from the laser measurements, is used to obtain an usable bed profile for the analysis. In the following sections the results of the tests are presented using this method.

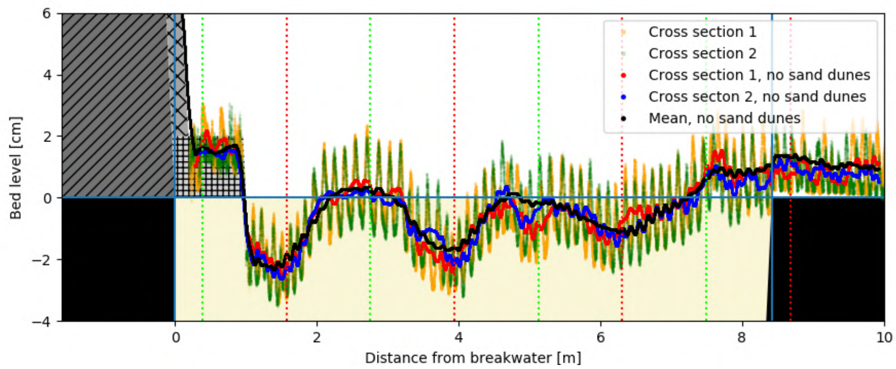

Figure 5.2: Processing scour data from the laser measurements. *Test 9*

5.1.1 Test series A

In test series A the impermeable structure is used as sloped embankment. The initial test was carried out with short waves and without a bed protection. No bed protection results in an abrupt transition between the rigid slope and the loose sand as can be seen in fig. 5.3a. Despite the abrupt transition, this did not cause a large amount of scour as can also be seen in fig. 5.3b. Some accretion even occurred close to the structure. During the test it was observed that sediment transport mainly appeared in the form of bed load transport. Suspended sediment could only be observed close to the bed and during the higher waves of the spectrum. While there was suspended sediment it was observed that sediment moved towards or away from the nodes and anti nodes as described by Xie (1981) in fig. 2.5. In fig. 5.3b it can be seen, that in the measured scour pattern, the first few nodes and anti nodes coincide with the corresponding peaks and troughs of the bed profile. Further away from the structure the scour pattern becomes chaotic at does not resemble a specific pattern anymore.

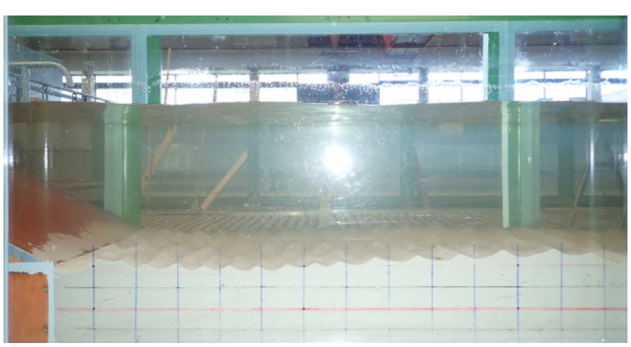

(a) Sideview after test, 1.5m width.

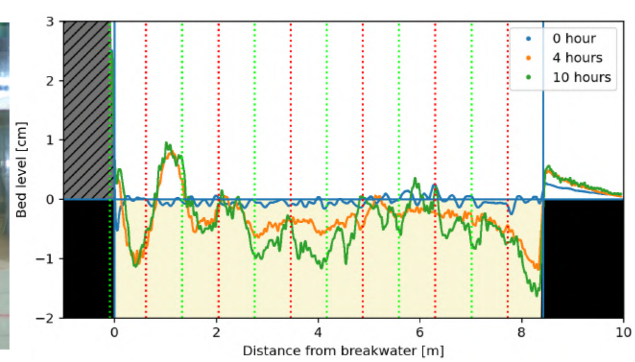

(b) Scour development over time.

Figure 5.3: Test A.1: $H_s = 0.14m$, $T_p = 1.6s$, *no bed protection.*

The second test in series A is similar to test the first one, except that a longer wave period (2.5s compared to 1.6s) is use and thus a longer wavelength. This results in a different node – anti node pattern and higher troughs and peaks in the bed profile, see fig. 5.4b. In this test the scour pattern follows the shape of a damping sine wave, similar to the results of Sumer and Fredsøe (2000) in fig. 2.7. During the test higher oscillating velocities could be observed as expected for longer waves. This also includes more sediment movement along the bed and slightly higher in the water column. Although, the suspended sediment was still only appearing during the larger waves. Furthermore, a large amount of sediment was transported offshore, as can be seen in fig. 5.4. Even though a peak was expected when looking at the node – anti node pattern, a large scour hole formed close to the structure. When the development of scour in time is considered it stands out that the nodes and anti nodes pattern is fully developed after a few hours. However, the maximum scour was increasing over time without reaching a equilibrium scour depth.

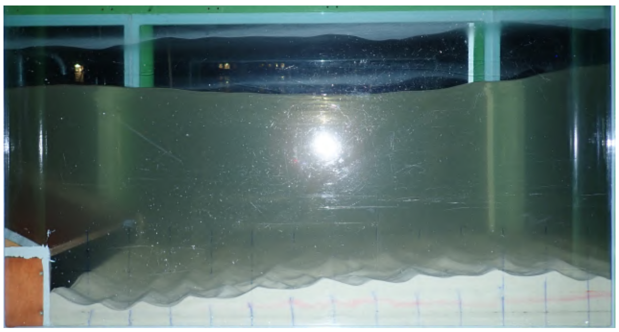

(a) Sideview after test, 1.5m width.

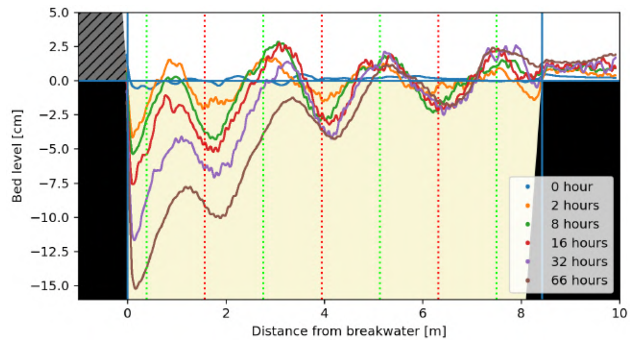

(b) Scour development over time.

Figure 5.4: Test A.2: $H_s = 0.14m$, $T_p = 2.5s$, *no bed protection.*

In the third test a toe was added to the structure, besides that the test was similar to test two. Since the hydraulic conditions did not change, it is logical that the scour pattern is fairly similar to test two. The bed protection, in form of a toe structure on top of a filter layer, covers the first 25 centimetre of the bed, fig. 5.5a. Compared to test two the first scour hole is further away from the structure and smaller, since part of it is protected. However, the second scour hole is deeper and similar in depth compared to the first scour hole in test two. When the first scour hole is considered in detail, it can be seen that stones from the toe structure and filter layer rolled into the scour hole. This creates an extended protective layer which is less thick than the toe structure. The test also shows a large amount of sediment transported offshore, most of it coming from close to the structure. Finally, the scour development over times shows a similar behaviour as test 2. The node and anti node pattern is fully developed, while the maximum scour depth keeps increasing.

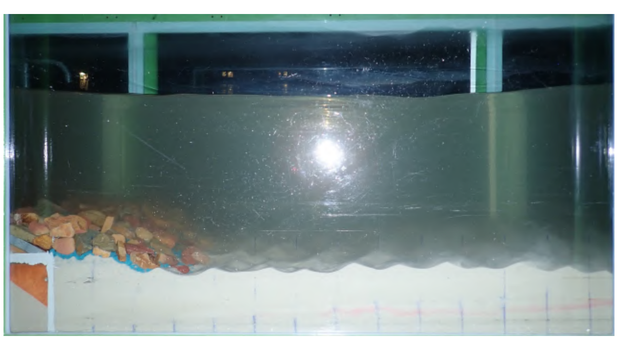

(a) Sideview after test, 1.5m width.

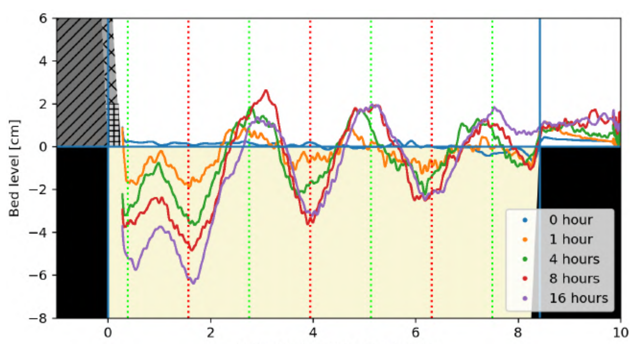

(b) Scour development over time.

Figure 5.5: Test A.3: $H_s = 0.14m$, $T_p = 2.5s$, *toe structure width* $= 0.25m$, *no additional bed protection.*

Test A.4 was performed using a long bed protection ($W_{b,p}$) with a length of 1.0m, including the same toe structure as used in test three. The total bed protection length ($W_{b,t}$) related to the wavelength is 3/8. The Again using the same hydraulic conditions and therefore a similar scour development pattern can be seen. Since a long bed protection is used, the scour hole closest to the structure in tests two and three is covered. In fig. 5.6b it can be seen that the first scour hole is in this test at the location of the first anti-node. This results in a relatively deep scour hole compared to earlier tests. This also means that the slope of the hole is quite steep, which can be seen in fig. 5.6a. The slope was covered with the bed protection, which has slid into the hole, similarly as the toe structure in test three. Finally it stands out that, again, a large amount of sediment is transported offshore.

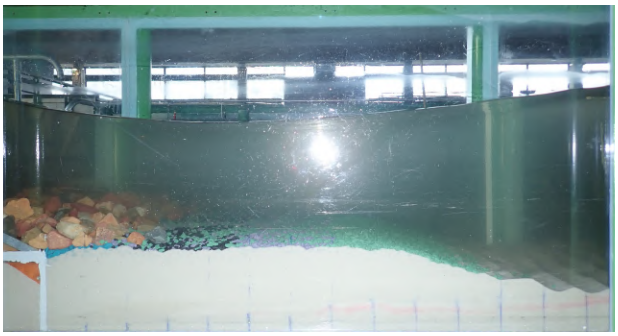

(a) Sideview after test, 1.5m width.

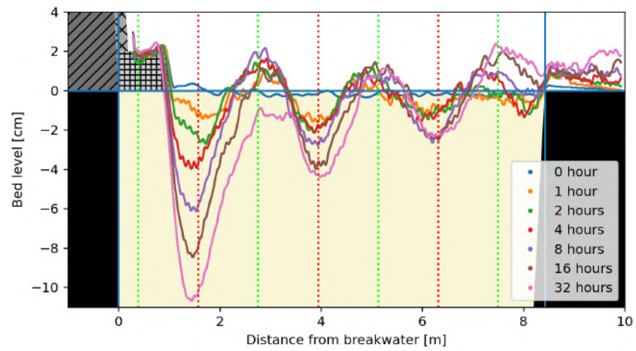

(b) Scour development over time.

Figure 5.6: Test A.4: $H_s = 0.14m$, $T_p = 2.5s$, *toe structure width* = $0.25m$, *total bed protection width* = $1.0m$.

The final test of the first series is a combination of test one and three. Using only a toe structure as bed protection just as in test three and shorter waves just as in test one. In this test, a large amount of sediment was transported from the most offshore part of the sand pit towards the structure, fig. 5.7b. This was partly due to the extremely long duration of the test. The scour pattern is only related to the wavelength when considering the bed profile close to the structure.

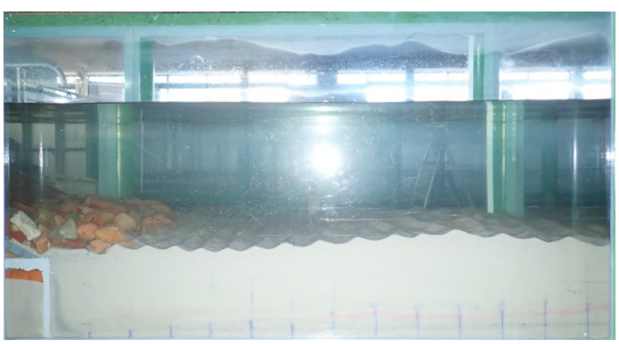

(a) Sideview after test, 1.5m width.

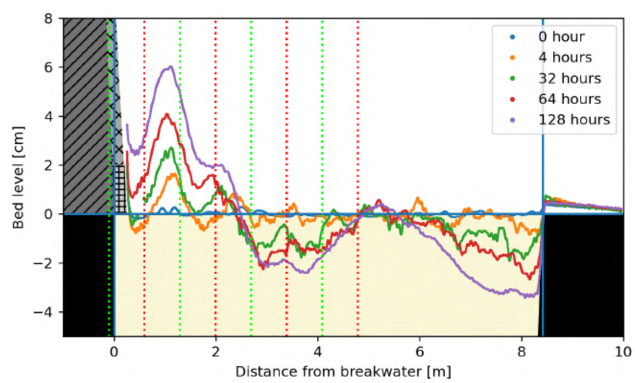

(b) Scour development over time.

Figure 5.7: Test A.5: $H_s = 0.14m$, $T_p = 1.6s$, *toe structure width* = $0.25m$, *no additional bed protection.*

5.1.2 Test series B

In test series B test were performed using a permeable breakwater as structure. The scale of the axis is equal in all the scour development graphs and can therefore be easily compared. The first tests of the series was done without bed protection as can be seen in fig. 5.8a. In this test the scour was much less compared to test series A. Especially the amount of scour close to the structure was a significant difference. The scour pattern shows the earlier mentioned damping sine wave, although some deformation of this pattern was visible at the boundaries of the sand pit. Besides the sine wave, an almost uniform loss of sediment was occurring from the sand pit to offshore. It is interesting to see that the third scour hole was deeper than the first and second scour hole, which was not the case in the same test with a impermeable structure.

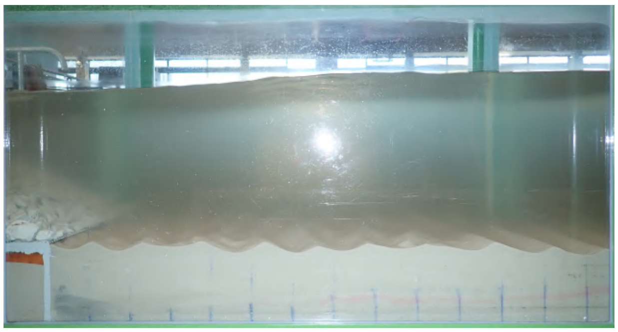

(a) Sideview after test, 1.5m width.

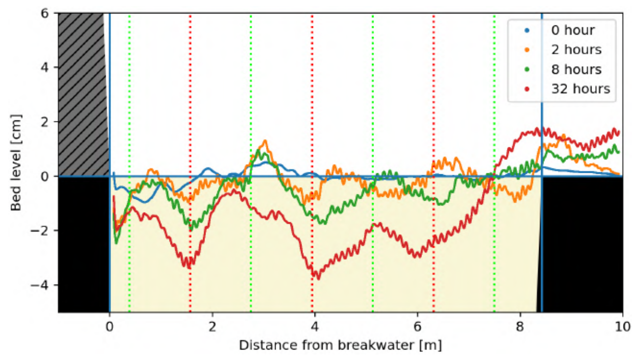

(b) Scour development over time.

Figure 5.8: Test B.1: $H_s = 0.14m$, $T_p = 2.5s$, *no protection*

In the second test (B.2) in the series a toe structure was added, besides that it was similar to test one of this series. Comparable to test series A, the toe structure (including filter layer) protects the first $25cm$ of the bed, fig. 5.9a. In this test the toe also reduces the depth of the first scour hole compared to the test without toe structure. The second scour hole had a similar depth compared to the second scour hole in the first test of this series. Besides that the third scour hole was again deeper than the first and second scour hole. In this test the damping sine wave was even better visible, especially after 16 hours of testing, fig. 5.9b.

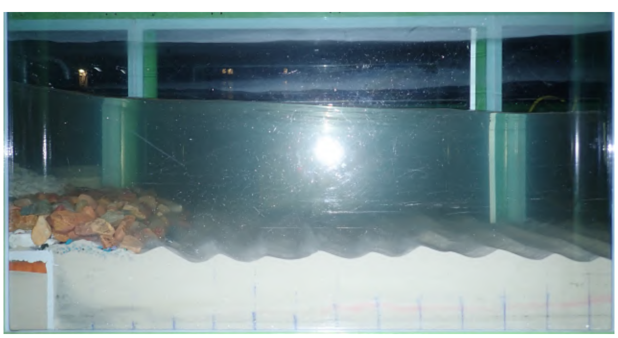

(a) Sideview after test, 1.5m width.

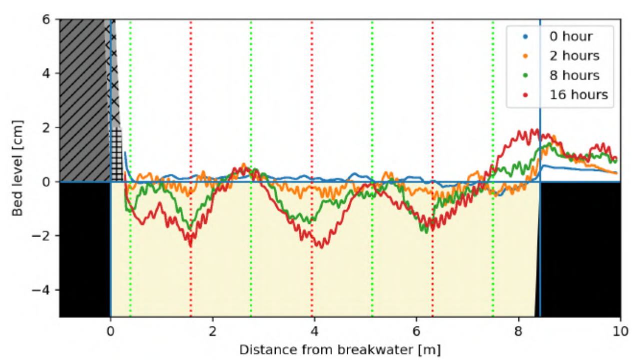

(b) Scour development over time.

Figure 5.9: Test B.2: $H_s = 0.14m$, $T_p = 2.5s$, *toe structure width* $= 0.25m$, *no additional bed protection.*

Test B.3 was used to research a higher wave height. Since the wave period was not varied, this also resulted in a steeper wave. For this test the steepness was $S_{o,p} = 1.7$, while for the . A toe structure is used to protect the bed similar as in test B.2. During the test it could be seen that a relatively large amount of sediment was displaced in the oscillating flow, compared to other tests in series B. In fig. 5.10b it can be seen that the first scour hole in this test is relatively steep. As consequence, a number of stones of the filter layer and toe slid into the scour hole, fig. 5.10a.

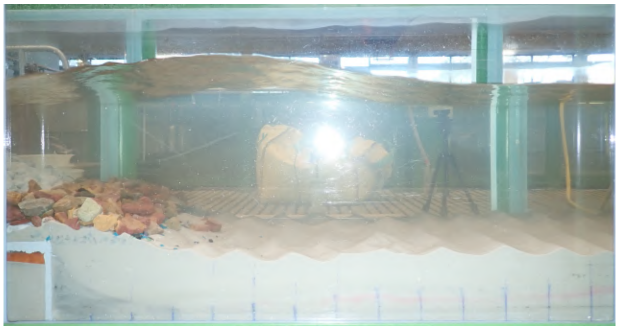

(a) Sideview after test, 1.5m width.

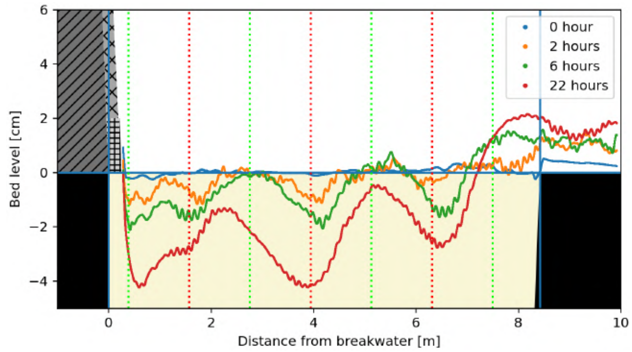

(b) Scour development over time.

Figure 5.10: Test B.3: $H_s = 0.18m$, $T_p = 2.5s$, *toe structure width* $= 0.25m$, *no additional bed protection.*

Test B.4 follows on test B.1 and B.2 using the same hydraulic conditions. However, the bed protection ($W_{b,p}$) was $1.0m$ long which the same bed protection as used in test A.4. The total bed protection length ($W_{b,t}$) related to the wavelength is 3/8. This results of this test are also in line with previous tests. Compared to test A.4 the sediment transported offshore is much smaller, especially close to the structure, fig. 5.11b. Similarly to test A.4 however, the bed protection does cover the first scour hole. Besides that, the scour hole at the location of the first anti node is larger compared to tests B.1 and B.2. The bed protection also slid into the scour hole as can be seen in fig. 5.11a. Finally it can be seen, in the same picture, that the bed protection did not displace at all. This becomes clear from the fact that the different colours used in the protection are not mixed in fig. 5.11a.

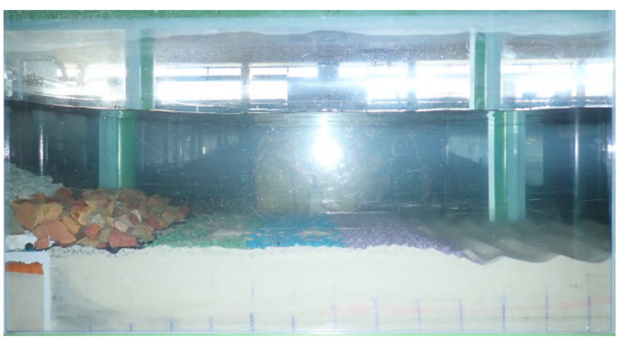

(a) Sideview after test, 1.5m width.

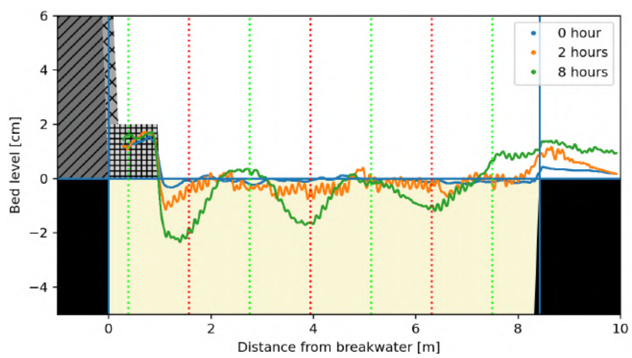

(b) Scour development over time.

Figure 5.11: Test B.4: $H_s = 0.14m$, $T_p = 2.5s$, *toe structure width* $= 0.25m$, *total bed protection width* $= 1.0m$.

The final test, B.5, was a repetition of test B.2 with the same toe structure and hydraulic conditions. This test was conducted to research the precision of these test. This is important since numerous aspects, such as the toe structure, are placed manually in these tests and could therefore lead to placement errors. In fig. 5.12b it can be seen that the first scour hole is small, while the second and third are deeper and similar to each other. Besides that it can be seen the some sediment is transported offshore. The shape of the bed profile is comparable to a damping sine wave, comparable to earlier results.

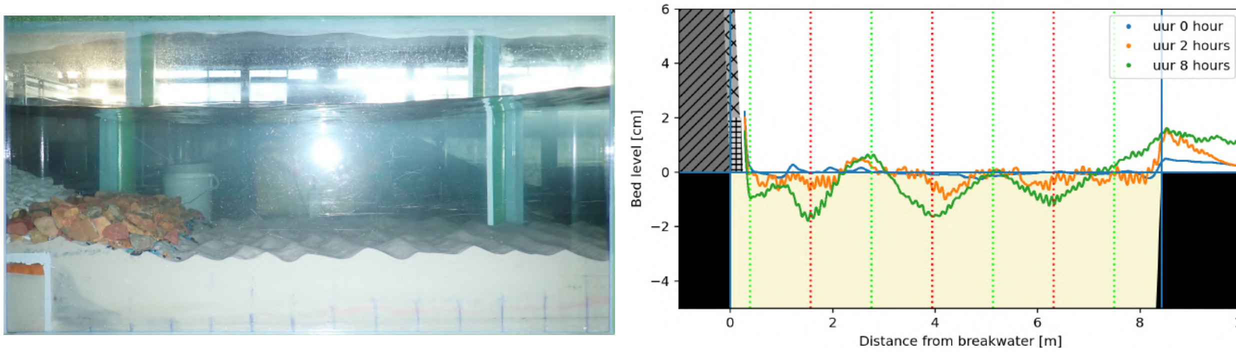

(a) Sideview after test, 1.5m width.

(b) Scour development over time.

Figure 5.12: Test B.5: $H_s = 0.14m$, $T_p = 2.5s$, *toe structure width* $= 0.25m$, *no additional bed protection.*

5.2 Photo measurements

During the tests cameras were used to make photos at specific time intervals. The pictures at the end of each are shown in the previous section, section 5.1. Besides that, the pictures at a time interval of one hour are used to present the development of scour over time close to the structure. The flume is supported every $1.5m$ preventing a clear view into the flume. Two cameras can capture up to $2.95m$ of the wave flume. In these results the first $2.0m$ from the embankment are considered, with a small section missing between $1.35m$ and $1.50m$. For the laser measurements a correction was done to remove the small ripples. For these results from the photo measurements the deepest point is used, excluding ripples. Thus, the photo measurements can be related to the laser measurements.

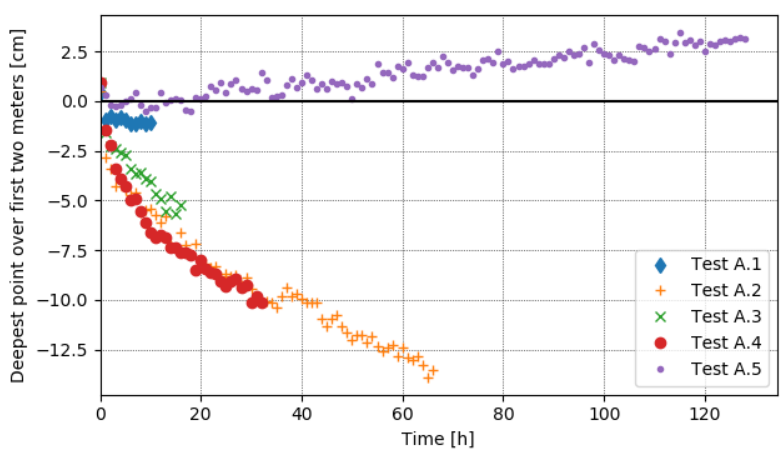

Figure 5.13: Maximum scour depth development over time, test series A.

The results of test series A are presented in fig. 5.13. Test A.2 - A.4 show a similar and clear pattern. At the start of the tests the scour increases rapidly, while after some time the rate of scour decreases. It stands out that in not a single one of the tests a equilibrium scour depth is achieved. Besides that it can be seen that while the bed protection has a large influence on the location of scour, section 5.1, it does not influences the depth of the scour hole. This since test A.2 did not have bed protection and test A.4 had a long bed protection of $1.0m$, while both tests show a similar scour depth.

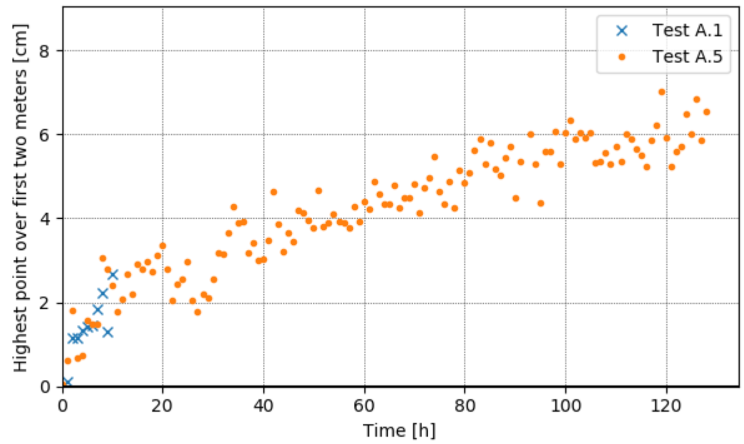

Figure 5.14: Maximum accretion development over time, test A.1 and A.5.

In test A.1 and A.5 accretion took place close to the structure, so the maximum 'scour' was not relevant. Therefore, the maximum accretion in these test is presented in fig. 5.14. It can be seen that test A.1 was relatively short and test A.5 was relatively long. Therefore, only the first few hours can be compared, which show a similar pattern for both tests. When considering test A.5 it can be seen that the amount of accretion per hour is decreasing over time. However, even after 128 hours, an equilibrium was not yet reached.

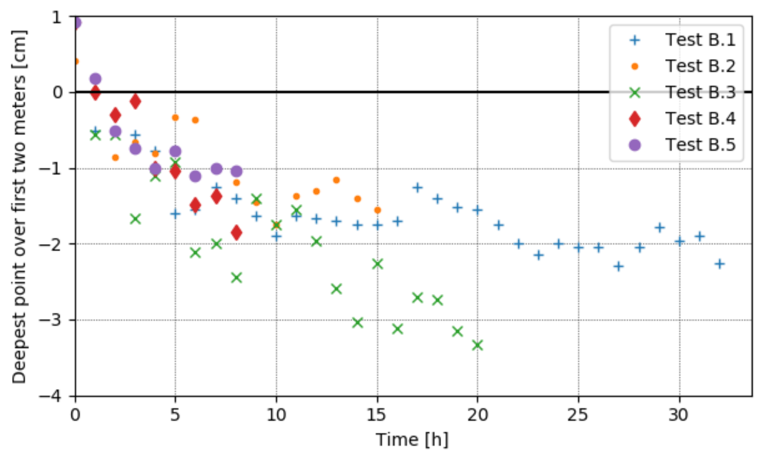

Figure 5.15: Maximum scour depth development over time, test series B.

In fig. 5.15 the results of test series B are presented. These tests, with a permeable structure, show more dampening of the scour per hour compared to test series A. Only in test B.3, in which a higher wave was used, a larger amount of scour can be seen. The other four tests show a comparable trend for the scour development. Similarly as in series A, the scour depth is not influenced significantly by the amount of bed protection, but the location of maximum scour is influenced.

Chapter 6

Analysis

In this chapter the results from chapter 5 are analysed. First, the different sediment transport processes are mentioned. After that the waves with a long wave period are analysed in detail. 8 out of 10 tests were performed with these long waves with a small wave steepness. Finally, steep waves with a short wave period are also analysed.

In this analysis the following five mechanisms of sediment transport and bed level formations are discussed:

- Small ripples.
- Standing wave scour patterns. (section 6.1.1 and section 6.2.1)
- Undertow (section 6.1.2)
- Scour due to downrush flow. (section 6.1.3 and section 6.2.3)
- Waves asymmetry / skewed waves (section 6.2.2)

In chapter 5, small ripples are mentioned and filtered out. Ripples are too small to consider in the scope of this research since they do not have an influence on the stability of coastal structures. The second and third mechanisms are discussed in chapter 2 and are considered important for the scour. Therefore, scour due to downrush flow and standing waves are analysed in detail. In the results, bed profile changes on a larger geometric and larger time scale can also be seen. The mechanisms causing these bed profile developments are expected to be, undertow or wave asymmetry.

6.1 Long waves

There is a large difference in bed profile development between the short and long waves, which is why these tests were analysed separately. Most of the tests (8 out of 10) were executed using the longer, $2.5s$ peak period, waves. These waves have a deep water $s_{o,p}$ of 1.4%, which corresponds to swell waves. In this section, the influence of these waves on the scour pattern is discussed. This contains earlier mentioned the mechanisms such as the downrush flow, standing wave scour patterns and undertow. Wave asymmetry / skewed waves is not discussed since the influence of this mechanisms could not be seen in these tests. In the figures in this section different tests are compared to point out the important scour mechanisms of these longer waves.

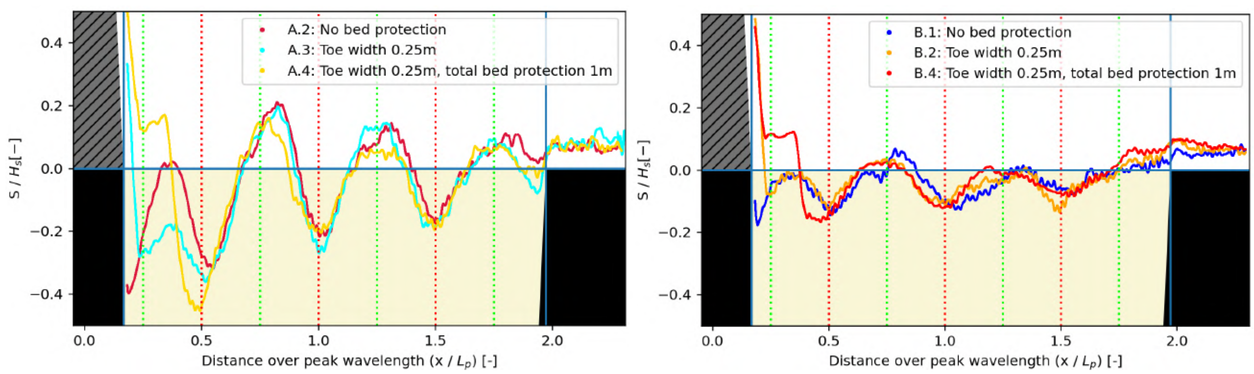

(a) Tests A.2, A.3 and A.4. *Impermeable structure.*

(b) Tests B.1, B.2 and B.4. *Permeable structure*

Figure 6.1: Influence bed protection on scour.

In both test series A and B, three tests are conducted to research the influence of bed protection on the scour pattern. All these tests are done using the same hydraulic conditions. In fig. 6.1 the dimensionless scour S/H_s of the two series is presented. When comparing the different tests in the figures, the following observations can be made:

- The scour pattern of the test series with a permeable and impermeable structure is very similar. The node and anti-node pattern follows the same damped sine wave in each test.
- The bed protection only influences the scour pattern close to the structure.
- The maximum scour depth is decreased minimally by a bed protection but its location does change.
- The scour hole closest to the structure appears directly when the bed protection stops. This suggests a downrush flow which causes this scour hole, following literature in section 2.3.
- The mean of the scour pattern with nodes and anti nodes/ bed level profile, is below zero in the graphs in both fig. 6.1a and fig. 6.1b. Even when excluding the first scour hole. This indicates a uniform loss of sediment to the offshore location which, can be caused by undertow due to breaking waves.
- Node and anti-node patterns follow the wave length based on the peak period T_p and not other wave period parameters such as $T_{m-1,0}$ or T_m. Besides that, the intersection between the water line and the structure slope must be used as reference for the distance from the embankment.

Thus, the bed protection mainly influences the location of maximum scour and the aforementioned downrush flow scour. The location of the first exposed part of the sand bed varies due to a different bed protection. The first part of the sand bed that is exposed is influenced by both the standing wave velocities and the downrush flow velocities. Since the node and anti node pattern follows a sine wave, these processes can either strengthen or weaken each others scour patterns. This results in a larger scour hole when longer bed protection ($1.0m$) is used, because the anti node coincides with the first exposed location of the sand bed. This scour hole is however, not close enough to the structure to cause instabilities. When no bed protection or only a toe structure is used, the scour patterns do not strengthen each other. The downrush flow in these cases is more important, because it is less damped by the long bed protection. The balance of these different processes determines the depth of the scour hole. In the tests in fig. 6.1 this resulted in similar scour depths for the same structure.

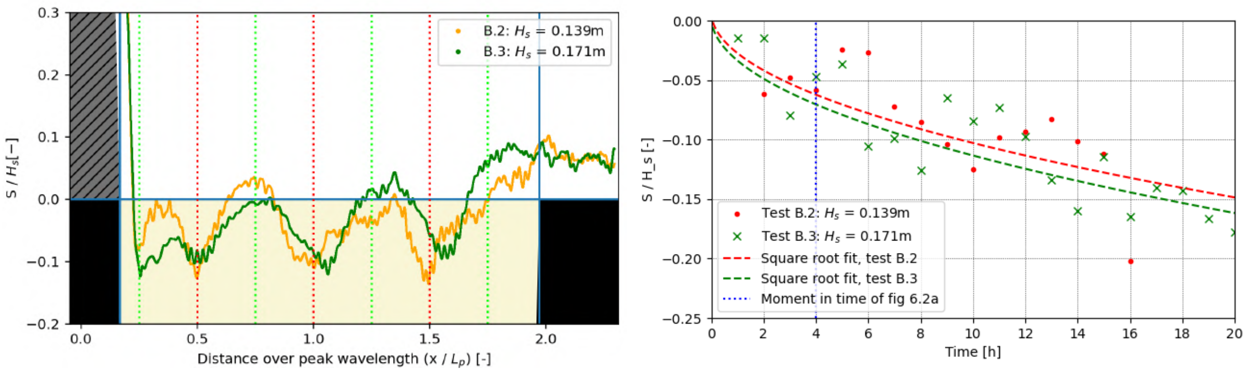

(a) Scour over wave height after 4 hours.

(b) Maximum relative scour in time close to the structure.

Figure 6.2: Influence of wave height on scour pattern.

Besides the variations mentioned earlier, test B.3 is performed to study the influence of the wave height. In test B.3 a H_s of $0.171m$ is used and this is compared to test B.2 where a H_s of $0.139m$ was used. In fig. 6.2 both tests are shown with a snapshot in time of the scour pattern and the maximum relative scour depth development in time. In fig. 6.2a it can be seen that the relative scour pattern of both tests is very similar. This is supported by fig. 6.2b in which the trend-line of the scour development is drawn for both test B.3 and B.4. In prior research done by Xie (1981), Sumer and Fredsøe (2000) and den Bieman et al. (2019) it was found that the scour has a linear dependency on the wave height. Although, this research only contains one variation on the significant wave height, the results of this variation support the findings of prior research.

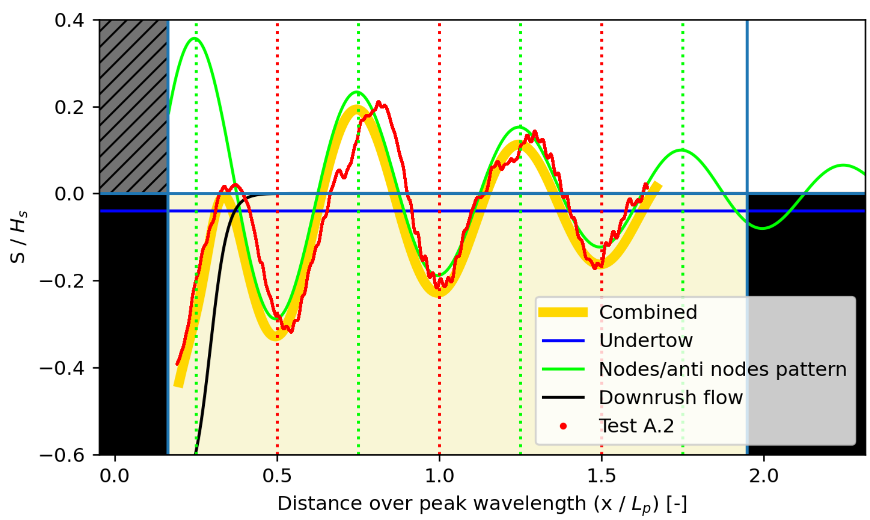

Figure 6.3: Different scour processes test A.2

6.1.1 Node and anti-node pattern

In fig. 6.3 the damping sine wave, downrush flow and undertow are shown corresponding to test A.2. The individual processes are similar to the measured scour profile when combined. For all other tests with waves with a H_s of $0.14m$, T_p of $2.5s$ and a $s_{o,p}$ of 1.4% the same processes influence the scour pattern. The differences between the tests are caused by a difference in either bed protection or reflection. The downrush flow is influenced by both, while the node and anti node pattern is only influenced by the reflection. Thus, the most important parameter for the node and anti-node pattern is the reflection. The reflection is mainly influenced by the permeability and the wave period in this particular research, because the slope angle was kept constant. In this section only waves with a period of 2.5s and a $s_{o,p}$ of 1.4% are considered.

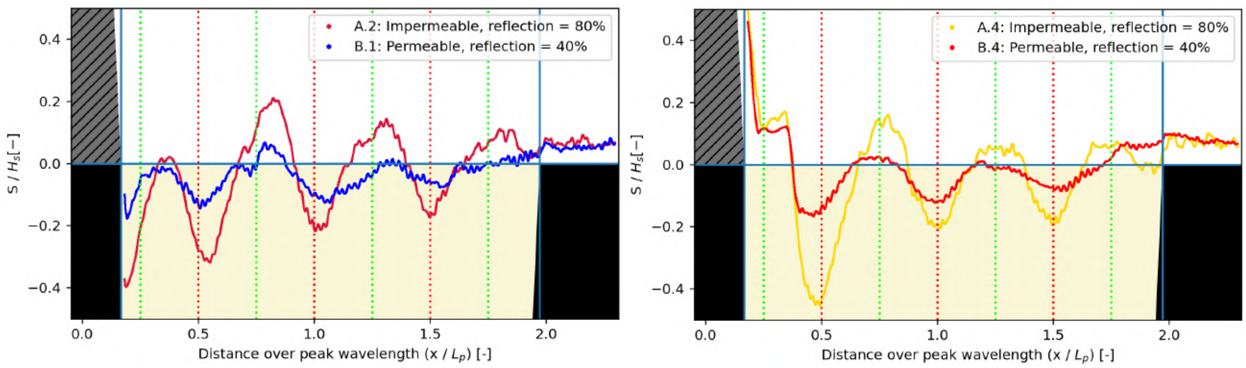

(a) Tests A.2 and B.1. *No bed protection*

(b) Tests A.4 and B.4. *Toe structure and bed protection.*

Figure 6.4: Influence permeability/ reflection on scour. *Test duration 8 hours.*

The influence of the permeability of the structure, and thus indirectly the influence of the reflection, is shown in fig. 6.4. In this figure, two different graphs are presented, one with bed protection and the other without. Both graphs show a test with an impermeable structure and a test with a permeable structure. It is clearly visible that the amplitude of the scour pattern is decreased significantly due to a lower reflection. To relate the node and anti-node pattern to the reflection the following assumptions and observations are made and listed below:

- The amplitude of the node and anti-node pattern is largest close to the structure. The amplitude decreases as the distance to the structure increases.
- The amplitude of the node and anti-node pattern stops increasing after approximately 8 hours of testing. This is equal to 12.000 waves when the T_p is used to determine the number of waves.
- The maximum amplitude of the node and anti-node pattern is defined by Xie (1981) in eq. (6.1) for the case of total reflection (vertical wall). It is assumed that the maximum amplitude relates to 100% reflection and that without reflection, no node and anti-node pattern is visible.
- The length scale of the node and anti-node pattern is equal to half the local peak wavelength (L_p).

$$\frac{S_{max}}{H_s} = \frac{0.3}{(\sinh \frac{2\pi h}{L_p})^{1.35}} \tag{6.1}$$

When using eq. (6.1) it can be found that the maximum amplitude of the scour pattern for the used wave is approximately $0.7S/H_s$. For the tests in this research the maximum amplitude is approximately $0.4S/H_s$ for 80% reflection and $0.1S/H_s$ for 40% reflection. Thus when comparing a reflection coefficient of 0.8 and 0.4, the amplitude of the node and anti-node pattern is four times lower for 40% reflection compared to 80% reflection. These findings, implicate a relation where the maximum amplitude of the scour pattern relates to, the maximum scour found using eq. (6.1) times the reflection coefficient squared.

Besides the reflection coefficient, the damping sine wave from fig. 6.3 is described by a decreasing factor in time and in space. A longer test duration relates to a higher amplitude of the node and anti-node pattern. And a larger distance from the structure relates to a lower amplitude of the node and anti-node pattern. The definition of the decrease of amplitude in space and the increase of amplitude in time are both determined empirically. When the scour in time is considered it is found that the amplitude of the node and anti-node pattern stops increasing after 12.000 waves. Thus, this can be considered as an equilibrium situation for the node and anti-node scour pattern.

These findings are combined in eq. (6.2), in which x is the distance along the x-axis relative to the peak wavelength (T_p) and measured from the intersection of the waterline and the structure slope. The damping factor is determined for the tests with a long wave period (T_p) of 2.5s. The factor "-0.85" is thus an empirical factor and determined for only one wave period. The influence of the duration is added by relating the number of waves to the maximum number of waves for which this scour pattern increases. The maximum for this value is equal to 1. In fig. 6.5 the derived empirical equation is plotted with the measured scour pattern. It can be seen that the node and anti-node pattern is represented quite well. Besides that it can also be seen that a scour close to the structure and a overall loss of sediment is not yet described. In the following sections the downrush flow and the undertow are discussed to complete the analysis on the scour pattern of the long swell waves.

$$\textit{For } \frac{N}{N_0} \leq 1 \textit{ and } N_0 = 12000\textit{:}$$

$$\frac{S(x,N)}{H_s} = S_{max} e^{(-0.85x)} \cos(4\pi x) K_r^2 \sqrt{\frac{N}{N_0}} \tag{6.2}$$

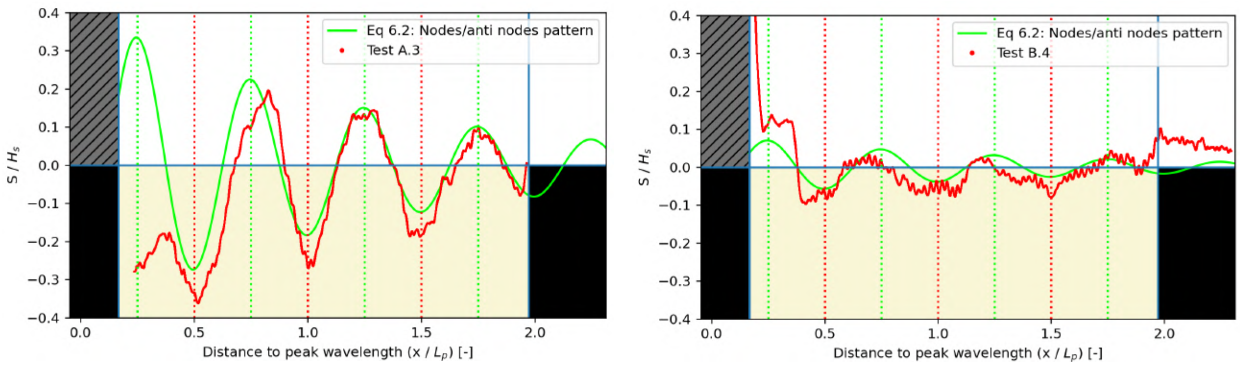

(a) Test A.3 after 8 hours.

(b) Test B.4 after 4 hours.

Figure 6.5: Fitted function compared to test results.

6.1.2 Undertow

A different mentioned process which influences the scour is the uniform sediment loss seen in the tests. In fig. 6.7 the volume change per meter width of the flume is presented. This is the loss over the first 7.5m of sand bed. It can be seen that this process for the different tests with varying structures is very similar. This indicates that the structures do not influence the sediment loss to offshore. A viable explanation for this is that the undertow caused by breaking waves on the foreshore is transporting sediment offshore.

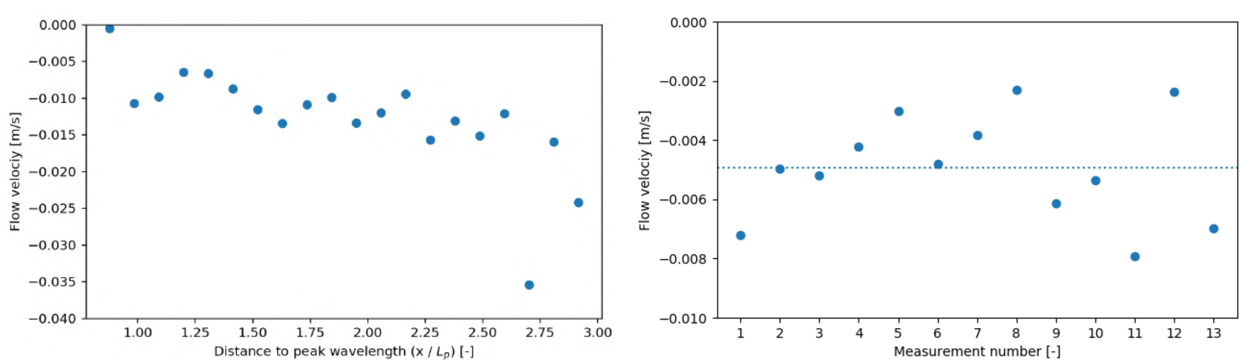

(a) Flow velocity at different locations.

(b) Precision flow velocity.

Figure 6.6: Flow velocity at 10cm distance from the original bed, test B.1. *Negative flow is offshore directed.*

To get a better understanding of the sediment behaviour in the experiments some additional flow measurements were performed. In test A.4, A.5 and B.1 the flow velocity was measured at $10cm$ above the original bed. Especially for the large scale sediment transport this can give more insight. The mean flow over 5 minutes, 120 waves, of testing is determined at different locations during test B.1, the results of these measurements are shown in fig. 6.6a. In this figure a negative flow velocity is offshore directed. From this can be concluded that over the whole length of the sand bed a offshore flow is present. This supports the hypothesis that a undertow is present during these tests which causes the uniform loss of sediment.

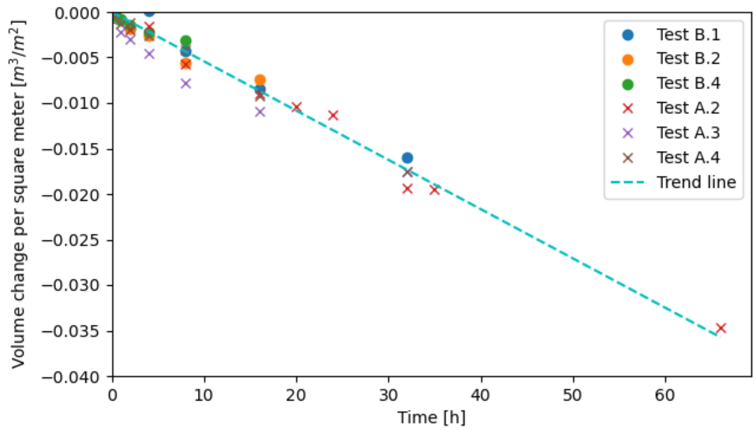

Figure 6.7: Volume change for waves with a $s_{o,p}$ of 1.4%.

The value of this undertow can not be determined, because the precision of the mean flow measurements is low. In fig. 6.6b it can be seen that when the mean flow velocity is determined multiple times at a location, it does not give a clear results. The results varied between $0.002m/s$ and $0.008m/s$ for this test. Although the flow velocity does not show a clear result, the measurement of sediment loss is more consistent. In fig. 6.7 it can be seen that the total loss of sediment is constant in time for tests with the longer wave period of $T_p = 2.5s$ and $s_{o,p} = 1.4\%$. This volume loss results in a average scour of 0.00054m or 0.54mm per hour.

6.1.3 Downrush flow

The scour due to downrush flow is dependent on both the permeability of the structure and the bed protection length. The downrush flow itself depends on more parameters: the surf similarity parameter, permeability of the structure, the roughness of the slope, water depth, toe structure and bed protection length. The effect of permeability has been discussed in section 6.1.1. Since the initial scour hole close to the structure is relatively deep, this changes the water depth. From which follows, that the downrush flow is dependent on the scour due to downrush flow. Because of this dependency, the scour due to downrush flow has to be calculated numerically.

However, without extensive calculation it can already be concluded that the roughness/ permeability of the structure and the bed protection length have a large influence. For the influence of the bed protection length, a quantitative influence has not been found. The bed protection causes the downrush scour to be relocated from the structure to further offshore. Besides that, a longer bed protection causes a decrease in downrush scour. Thus the longer the bed protection, the further away and smaller the scour hole becomes.

Structure type	γ_f
Concrete, asphalt and grass	1.0
Pitched stone	0.80–0.95
Armourstone - single layer on impermeable base	0.7
Armourstone - two layer on impermeable base	0.55
Armourstone - permeable base	0.4

Table 6.1: Roughness reduction factor, Dont and Laborie (2007); Van der Meer (2002)

The influence of the roughness and permeability of the structure is described with a roughness reduction factor. For the roughness of the structure γ_f is used as roughness reduction factor for processes as run-up or overflow in Dont and Laborie (2007); Van der Meer (2002). This roughness factor is mostly influenced by the permeability of the structure. When the permeable and impermeable structure are compared this roughness factor can be used to relate the amount of downrush flow scour. The roughness factor for a impermeable flat slope is equal to 1, while the roughness factor for a permeable breakwater slope is equal to 0.4. For all three sets of two tests which are compared, the ratio between the two roughness factors is equal to the ratio between the downrush flow scour.

6.1.4 Reproducibility

Test B.10 is performed as repetition test to study the precision and reproducibility of the tests in this research. During the execution of the tests the sand bed, toe structure and bed protection are manually placed. This can cause inaccuracy's at the beginning of the test, which could be magnified during testing. In fig. 6.8 the results of this test is presented. Both the maximum scour in time, fig. 6.8b, and the scour after 8 hours, fig. 6.8a, show a similar result for both tests. Although single measurements of the maximum scour depth in time can differ up to 0.03 S/H_s, the trend line is very similar. The same holds for single scour measurements on a location, the scour pattern is very similar while a single measurement can differ up to 0.05 S/H_s between tests.

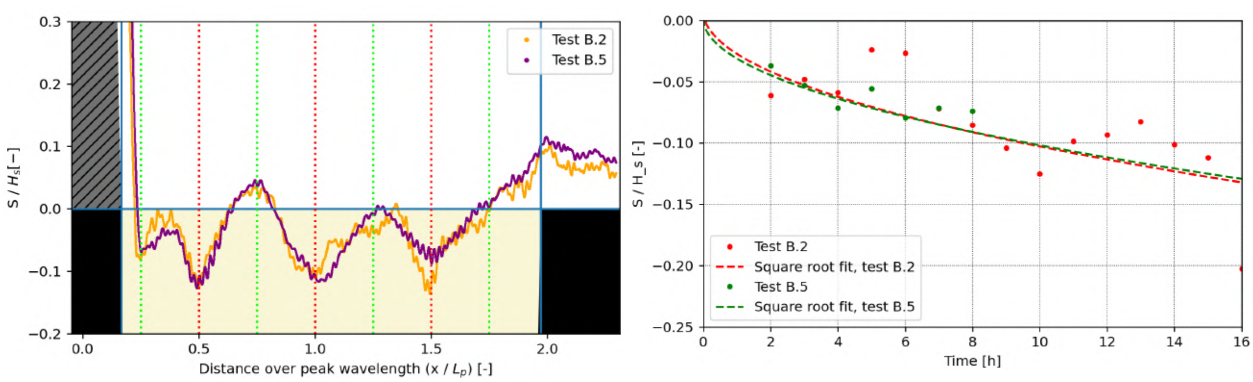

(a) Scour over wave height after 8 hours.

(b) Maximum scour in time within $0.5L_p$ of the structure.

Figure 6.8: Repetition test B.2 and B.5

6.2 Short/steep waves

In this research two tests are performed with short (T_p = 1.6s) and steeper ($s_{o,p}$ = 3.5%) waves. The difference is that test A.1 was performed without using a bed protection or toe structure, while test A.5 was executed with a toe structure. In this section the test are related to the earlier described scour processes. For these tests the standing wave scour pattern, wave asymmetry/ skewed wave and the return flow are considered. The undertow is not discussed, since the influence of this mechanism could not be seen in the tests.

6.2.1 Node and anti-node pattern

In section 6.1.1 the node and anti-node patterns are discussed in detail. In this section the relation between short waves and the standing wave scour pattern is related to the finding in section 6.1.1. The node and anti-node pattern is for steep less distinctive than for longer, less steep, waves. In fig. 6.9 the proposed eq. (6.2) is used to show the estimated scour. What becomes clear is that the scour measured scour has a more chaotic pattern. The amplitude of the node and anti-node pattern is still valid. However, the location of the troughs and peaks has no clear relation to the node and anti-node pattern.

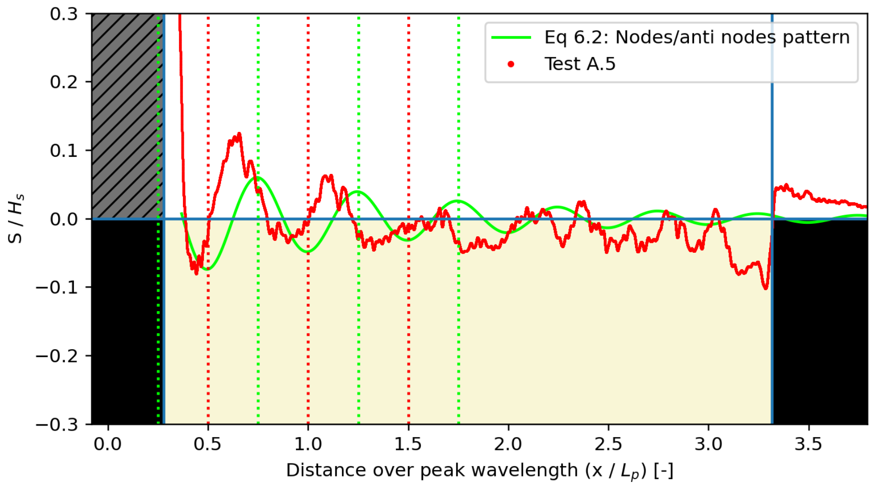

Figure 6.9: Scour pattern short/steep waves (T_p = 1.6s, $s_{o,p}$ = 3.5).

6.2.2 Waves asymmetry / skewed waves

It stands out that close to the structure the bed profile shows a larger accretion than erosion. If the scour development over time in test A.5 is considered it can be seen that the scour close to the structure grows slowly over time, fig. 6.10b. This long duration is not realistic when storm conditions are considered, but for less extreme conditions this time scale is possible. A process which is known for onshore sediment transport is the asymmetry of the wave movement. This is a large scale process, which corresponds to the long time scale of the sediment behaviour in these two tests.

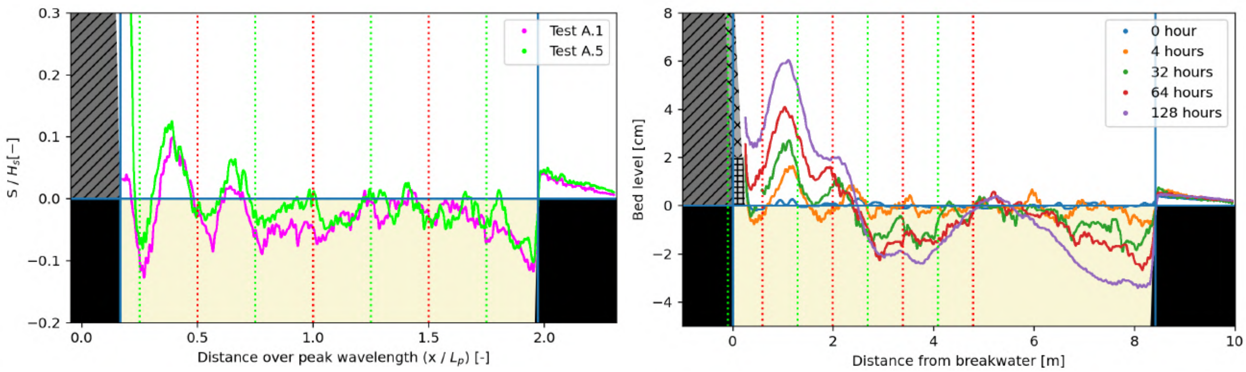

(a) Scour pattern short wave.

(b) Scour development in time test A.5

Figure 6.10: Scour development over time.

6.2.3 Downrush flow

For the steeper, $s_{o,p} = 3.5\%$, waves the downrush flow is also causing scour close to the structure. Although, the effects are much smaller compared to the longer waves. The maximum scour depth of the first scour hole, which is influenced by the downrush scour, is four times smaller for the steeper waves. The maximum scour depth is significantly less for the shorter wave period. The sinusoidal scour pattern is less clear as for the longer wave period. However eq. (6.3) still gives a good description of the maximum scour depth for a test duration up to 12000 waves.

6.3 Empirical scour equations

In prior research by den Bieman et al. (2019); Sumer and Fredsøe (2000) empirical equations are used to quantify the amount of scour. In this section the data acquired in this research is compared to existing literature. In fig. 6.11 the most recent study done by den Bieman et al. (2019) is shown. The used structure and hydraulic conditions are very similar between this study and the study done by Den Bieman. Therefore both studies can be compared with minimal discrepancies. However, the following remarks should be noted:

- Most tests by Den Bieman were performed using 1000 waves, with one longer duration test of 3000 waves. In comparison, in this thesis all tests were done with more than 3000 waves.
- The wave steepness in this research is larger compared to the research done by Den Bieman. Reaching respectively from $s_{o,p} = 1.4 - 3.5$ and $s_{o,p} = 0.34 - 1.82$.
- In this thesis the used sand has a relative large grain diameter, $d_{n50} = 0.26mm$. This results in relative coarse sand according to the definition of Xie (1981), while in the study of Den Bieman relatively fine sand was used.

Besides the results of den Bieman et al. (2019), fig. 6.11 shows multiple measurements of each test in this research. The equation of den Bieman relates the dimensionless scour to the number of waves times the dimensionless wave height, dimensionless peak wavelength and the dimensionless water depth on the toe structure. For a small number of waves the results are similar in both studies. However, for larger number of waves ($N > 3000$) the equation as described by den Bieman is not valid. This since the maximum scour depth for a longer test duration does not follow a linear trend, but seems to dampen out. This also follows from the figure since it can be seen that the linear growth, as described by den Bieman, only complies with the results of this research for a short test duration (N < 3000).

A second comparison, relates the results of Sumer and Fredsøe (2000) to this research in fig. 6.12. In the research of Summer and Fredsøe most of the tests were performed with regular waves. The measurements

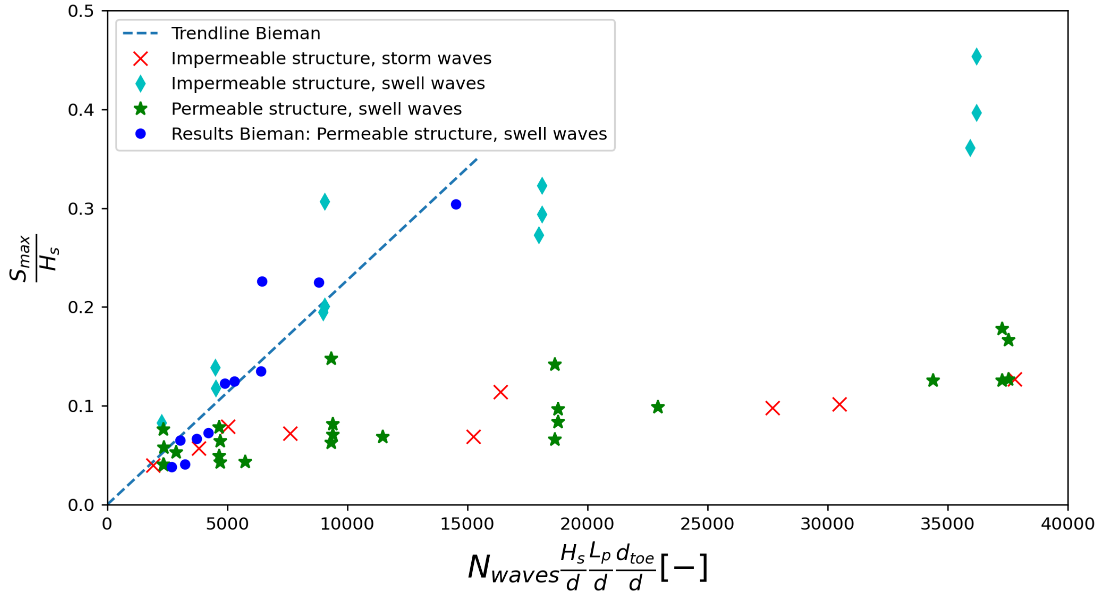

Figure 6.11: Comparison results with study of den Bieman.

which are shown are done using a permeable breakwater with a steeper slope of 1:1.75 and regular waves. They report that an equilibrium of scour was reached after ± 3000 waves. From Sumer and Fredsøe (2000) it can also be concluded that regular waves result in more scour than irregular waves. This is especially important for the node and anti-node pattern.

In fig. 6.12 the dimensionless scour is plotted against the local water depth over the local peak wavelength. The dimensionless scour in this research is determined using a significant wave height, while Sumer and Fredsøe (2000) used the wave height of regular waves. Summer and Fredsøe plotted the equilibrium scour depth which was reached at the end of the tests. From this research multiple measurements over time are plotted since a equilibrium scour depth has not been found. The amount of scour for both studies is in the same order of magnitude.

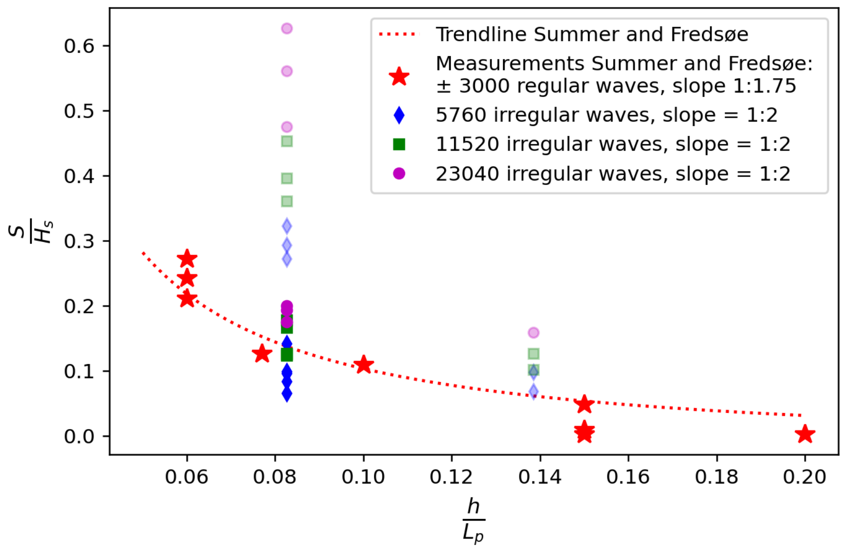

Figure 6.12: Comparison results with study of Summer and Fredsøe.
Transparent points: impermeable structure.

The last empirical equation which is used to compare the results to, is the derived equation in section 6.1.1. The maximum dimensionless scour depth at a certain moment in time is calculated instead of a whole scour pattern. To do this the cosine and the dampening factor are excluded and assumed to be equal to 1. From this eq. (6.3) follows for the maximum scour at a certain moment in time. Time is in this case represented by the number of waves.

For $N_0 = 12000$*:*

$$\frac{S(N)_{max}}{H_s} = \frac{0.3}{(\sinh\frac{2\pi h}{L})^{1.35}} K_r^2 \sqrt{\frac{N}{N_0}} \tag{6.3}$$

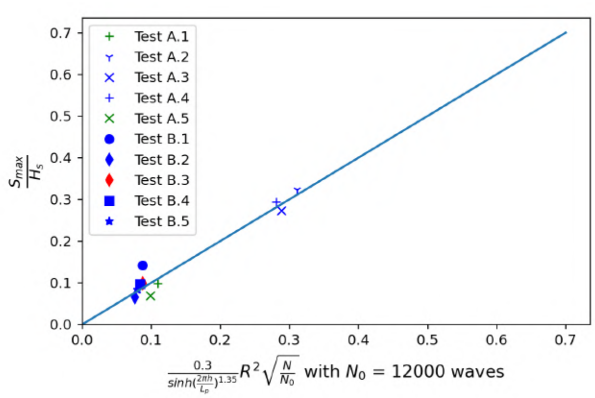

(a) Empirical fit after 4 hour

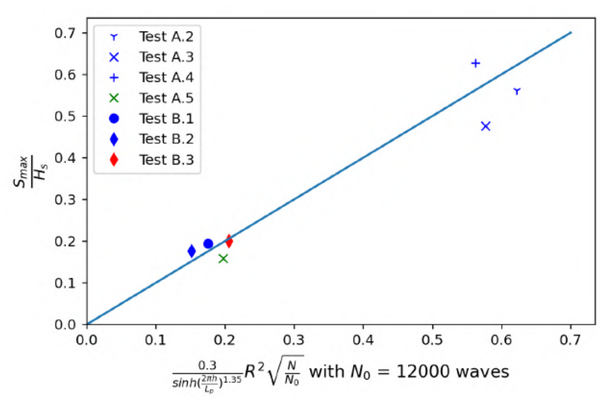

(b) Empirical fit after 16 hour

Figure 6.13: Empirical fit max scour equation after 4 and 16 hours

In fig. 6.13 the expected scour, calculated with eq. (6.3), and the measured scour are plotted after both 4 and 16 hours of testing. It can be seen that for all tests the prediction of maximum scour depth is quite good. Even though, the tests with a permeable and impermeable structure are shown combined with both short and long waves. Besides that, the individual scour processes are not represented in this equation. In fig. 6.14 scour measurements for more moments in time are plotted. It can be seen that even when more than 12000 waves, N_0, are used, the equation can still predict amount of scour. Thus, although the physical processes can not be distinguished in this equation, the results are viable. For more insight, some remarks about eq. (6.3) are made in the list below:

- The equation is based on an other empirical equation derived by Xie (1981). The maximum amount of scour depth was derived for a node and anti-node pattern in front of a vertical wall.
- The dampening factor is excluded, which causes the scour amplitude due to the node and anti-node pattern to be overestimated.
- Downrush flow and large scale processes such as, undertow and wave asymmetry are excluded.
- The root mean squared error of the measured dimensionless scour and the expected dimensionless scour of eq. (6.3) is equal to 0.035.

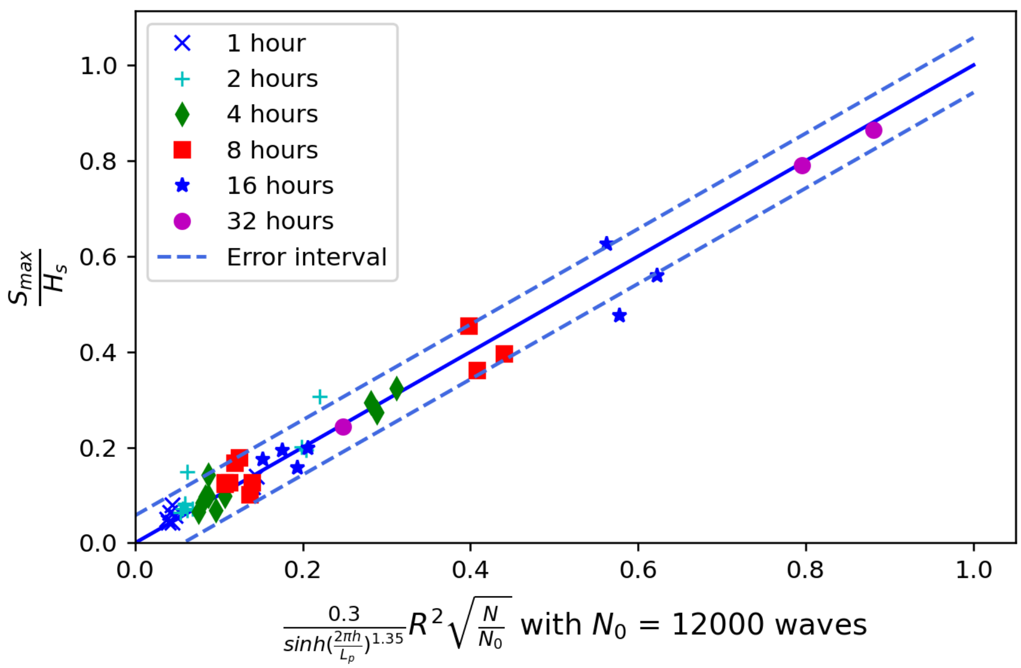

Figure 6.14: Empirical fit eq. (6.3) for maximum scour and 90% error interval.

Chapter 7

Discussion

This thesis is part of research into the scour in front of breakwaters and revetments. Specifically the influence of a bed protection is researched in more detail. In this thesis knowledge of the processes which causes this scour is improved. This section discusses some insights and processes which are important to consider for scour in front of a structure.

First of all, the length of the bed protection is discussed and the influence on the scour location. Since the bed protection moves the scour away from the structure, it is a very effective measure to prevent instabilities due to a scour hole close to the structure. However, it was also found that the maximum scour is not necessarily found when no bed protection is used. This since nodes or anti nodes can coincide with the downrush flow scour location. In reality many different wave spectra can occur with corresponding peak wavelengths. This also means that the location where the nodes or anti-nodes coincide with the downrush flow changes constantly. Consequently, the location of maximum scour is also not fixed. Therefore, the actual influence of a bed protection is very hard to determine.

However, When the wave conditions are more constant at a certain location the known node and anti-node pattern can be used to obtain an advantage. In this research it was found, that the location of the transition between the protection and the sand is were the downrush flow has the largest influence. On the other hand, the node and anti node pattern is dependent on the local wavelength. For designers the bed protection length can thus be used to move this location to a desirable place. When the governing wave conditions are known a design can be made in such way that the node and downrush flow scour coincide. This, to create a situation with minimal scour. In this research, a longer bed protection caused slightly more scour and only a toe structure would have sufficed. When more wave conditions are tested in future research, this could reduce the amount of bed protection significantly for breakwaters were scour due to waves is governing.

Another point of discussion for scour designs, is related to the design conditions of a structure. In this research it could be seen that short and steep waves caused deposition near the structure while longer waves caused scour. A design of a breakwater or revetment is normally based on storm condition or, which are high, short and steep waves or swell waves, which are long and not steep. Thus, the storm conditions which are often used, might not be the conditions with the maximum amount scour. From former research done by den Bieman et al. (2019) and Sumer and Fredsøe (2000) it also followed that long waves are related to more scour. Contrary to storm waves, long waves can be present for multiple days in a realistic situation. It is therefore important to not only consider a larger time scale, but also multiple wave conditions, specifically long waves.

Chapter 8

Conclusions

This chapter contains the most important findings of this research. Besides that, this chapter contains the research question from chapter 1, which are answered to conclude this thesis. First of all, the sub questions are answered individually. The answers of the sub questions combined answer the main research question.

Which parameters have an influence on scour in front of the toe structure of a sloped embankment and how are the parameters related to the scour?

In section 2.5 the parameters of influence according to existing literature are listed. This list contains dimensions of the sloping structure, toe structure and bed protection. Besides that it also contains sand properties, test duration and the hydraulic conditions. In this research not all of these parameters were varied to study there influence.

The permeability of the structure and the bed protection, which were the main focus in this thesis, are discussed in the next two sub questions. The significant wave height, peak wave period and the number of waves are discussed in the list below:

- **Significant wave height:** The scour in front of a structure is linearly dependent on the significant wave height. The larger the significant wave height, the larger the scour depth.
- **(Peak) wave period:** Scour in front of a embankment is strongly dependent on the wave period. From this research it can be concluded that a long wave ($s_{o,p}$ = 3.5) with a high period causes more scour than a short wave ($s_{o,p}$ = 1.4) with a low period. The short waves caused accretion at the toe of the structure.
- **Number of waves/ duration:** A higher number of waves causes more sediment to move and thus a larger accretion or erosion. The different scour processes show a different behaviour in time. However, combined this process starts linearly and after multiple hours of testing the scour in time decreases.

What is the effect of permeability of the structure on the scour depth?

A permeable structure has a lower reflection coefficient (40%) compared to a impermeable structure with a reflection of 80%. In this research the impermeable structure also has a rough slope. The rough slope causes a decrease in downrush flow and due to that also a decrease in scour. The roughness factor used in Dont and Laborie (2007) for overflow and run-up can also be used for downrush flow and the scour caused by this.

The lower reflection coefficient, due to the higher permeability, relates four times less scour for 40% reflection compared to 80% reflection. This scour is caused by a node and anti node pattern. The amplitude of this pattern is related to the reflection coefficient squared in the results of this research.

What is the influence of a toe/bed protection on the scour in front of a sloped embankment?

The bed protection, including a toe structure, influences the location of the first scour in the sand bed. A toe structure or bed protection shows no significant effect on the maximum scour depth for protection lengths smaller than one wave length. However, the longer the toe/bed protection, the further away the maximum scour depth occurs.

What is the equilibrium depth for a scour hole in front of a sloped embankment and which variables influence this?

In this research all tests were performed with at least 12.000 waves. Even though this test duration is relatively long, no equilibrium was found for the scour depth. The different scour processes have also a different behaviour in time. The node and anti node scour pattern does have an equilibrium depth. For long waves with a peak period of $2.5s$ this equilibrium is reached after approximately 12.000 waves. For short waves not a clear result could be found, this due to the fact that the nodes and anti nodes pattern was not clearly distinguishable. For the downrush flow scour, an equilibrium depth is not found in one of the tests with an impermeable structure. For the longer test with the permeable structure a equilibrium could be found after approximately 16 hours or 24.000 waves.

From which point in the structure or scour protection should the length of the total bed protection be measured?

The total bed protection length is from the point where the waterline crosses the slope of the structure to the end of the scour protection. The embankment, toe structure and scour protection are all protecting the bed against scour and replacing the scour further offshore.

Which wave period should be used to determine the wavelength and derive corresponding scour patterns?

The wavelength is an important parameter in relation to the amount of scour and the location of the scour. In this research it was found that the wave length based on the local water depth and peak wave period should be used to derive scour patterns.

Given the main objective of the research, how can a sand bed be modelled most accurately in a small scale model?

To model a sand bed in this research the sediment which should be used must be as small as possible while still having the properties of a sandy material without cohesion. The best material available for this is silica M34 sand, which has a d_{50} of $0.15mm$. This to create a scalable physical model with a non-cohesive sediment. Literature such as Frostick et al. (2011); Dont and Laborie (2007) also suggests that the smallest possible non-cohesive sand is the most accurate method to model a sand bed. Since sand with a d_{50} of $0.26mm$ was used in this research, it is recommended to test different sand diameters in future research as discussed in chapter 9.

What is the expected, wave induced, scour depth over time in front of a sloped embankment, and what is the effect of a scour protection on the (location of the) maximum scour depth.

The expected scour depth is for the larger part dependent on the parameters as discussed in the respond to the the first research question of this thesis. These parameters result in a few processes, namely: downrush flow scour, a damping sine wave pattern, undertow, asymmetric waves and sand dune development. Of these processes the downrush flow scour and the damping sine wave are the most significant. A quantitative approach for the damping sine wave due to a standing wave pattern was found. This relates both the number of waves and the location to the amount of scour in eqs. (8.1) and (8.2). This process does not influences the location of the maximum scour depth, but only the amount of scour. eq. (8.2) is derived by Xie (1981) for the maximum scour, due to standing waves, in front of a vertical breakwater.

$$\frac{S_{max}}{H_s} = \frac{0.3}{(\sinh \frac{2\pi h}{L})^{1.35}} \tag{8.1}$$

For $\frac{N}{N_0} \leq 1$ *and* $N_0 = 12000$*:*

$$S(x,N) = S_{max,v} e^{(-0.85x)} \cos(4\pi x) K_r^2 \sqrt{\frac{N}{N_0}} \tag{8.2}$$

Furthermore, a similar quantitative equation was determined for the maximum scour depth, eq. (8.3). This equation is also based on the maximum scour equation for a vertical wall by Xie (1981). The influence of the reflection is added to consider other structures besides vertical walls. This results in a equation which is valid for both vertical and sloping structures. This is an added value to the existing literature on scour, such as the scour manual by Hoffmans and Verheij (1997), which mainly focuses on vertical walls.

For $N_0 = 12000$ *and* $\frac{x}{L} < 1$*:*

$$\frac{S(N)_{max}}{H_s} = \frac{S_{max,v}}{H_s} K_r^2 \sqrt{\frac{N}{N_0}} \tag{8.3}$$

The location of maximum scour is mostly influenced by the length of the scour protection. A longer scour protection causes the scour hole due to the downrush flow to be moved further offshore. If the location of the end of the bed protection coincides with a node the maximum scour is lower than without bed protection. However, if this location coincides with a anti-node the maximum scour can be higher than without scour protection.

Chapter 9

Recommendations

The scour in front of a sloped embankment is dependent on many different parameters, as was discussed earlier in this research. For future studies many different aspects could be varied to study either small or large influences. In this section the most important aspects are discussed which, when researched, would complete the knowledge gap needed to predict the amount of scour. A prediction, which would be valid for all kinds of embankments and bed protections. For this two important steps have to be taken: Firstly, additional physical model tests have to be done to collect more data. Secondly, the prediction of the scour processes have to be programmed into a numerical model.

In the analysis a formula was presented for the scour pattern due to standing waves. The number of waves, reflection, location, water depth, wave height and wavelength are all variable in this formula. Although, the scour due to long waves can be modelled by this, the equation is not proven to be valid for other conditions. To prove that this equation is valid for more than one conditions additional tests have to be executed. Besides that, the combination of downrush flow and the node anti node pattern is not yet fully described. The following knowledge gaps have to be filled to achieve this:

- The number of waves is varied by measuring at different time intervals. In this research the laser measurements were done after the following hours of testing: 0, 0.5, 1, 2, 4, 8, 16. For future research it might be useful to measure every hour to have a better insight in the decrease of scour in time. This is only needed for one or two tests, since the process does not change.
- An important aspect of the scour process are the wave conditions, since these are the driving forces. In this study and in earlier studies, it was concluded that the wave height has a linear relation with the scour. This is acknowledged widely and does not need further attention. But, for the wave steepness or wave period some extra data would be very useful. When the wave height is kept constant, the wave period and steepness vary in a similar manner. The wave steepness has a influence on the breaking parameter and on the reflection. The breaking on the structure influences the downrush flow, which is important for the scour. As said earlier, the downrush flow is still difficult to predict and thus this could fill part of this knowledge gap. Furthermore, the wavelength influences the nodes and anti nodes pattern. As discussed earlier, the location of these nodes and anti nodes coinciding with the downrush flow can have a significant impact. These two reasons show that a different wavelength/ steepness is useful to study.
- The permeability of the structure is included in both the reflection and the roughness coefficients. The influence of the reflection is understood quite good. However, the influence of the roughness factor on the downrush flow needs to bed better understood. This to be able to better predict this part of the scour process. To achieve this, an extra structure type can be tested with a different permeability.

- The bed protection length was one of the main focus points in this research. Yet, it is still a variable which could use more attention. This since, as said before, the location of the nodes and anti nodes and the downrush flow scour determine the maximum scour depth. When designing a test program this could be combined with varying the wavelength. When changing either the wavelength or the bed protection length a new situation for the scour location can be created. It is advised to perform a test were the end of the bed protection lies in the middle between a node and anti node. This could give a better insight on the downrush flow scour.

Besides these variations in the tests another important aspect can be changed. In this research "coarse" sand was used, which indicates mainly bed load transport. According to Xie (1981), fine sand causes a different scour pattern for vertical walls. Although vertical walls and sloping structures have different behaviour, a considerable part of the scour processes are similar. Besides that, when full scale structures are considered, sand is often relatively fine. This would mean that most of the sediment is in suspended transport instead of bed load transport. Therefore, it is important to study the effects of fine sand on scour in front of a sloped embankment.

If all the above mentioned variations are tested, a large and complete data set would be available. To use this up to full potential, a numerical prediction method is needed for scour in front of a sloped embankment. This numerical method is necessary to combine the different scour processes. Flow, is besides a driving force for scour, also depth dependent. Scour causes differences in depth and thus the flow is also, partly, dependent on scour. Therefore, a iterative process is needed, to fully resolve the scour problem. When this is done, the scour can be predicted in both time and space.

References

Borsje, B., Kranenburg, W., Roos, P., Matthieu, J., and Hulscher, S. (2014). The role of suspended load transport in the occurrence of tidal sand waves. *Journal of Geophysical Research: Earth Surface*, 119(4):701–716.

den Bieman, J. P., van Gent, M. R., and Hoonhout, B. M. (2019). Physical model of scour at the toe of rock armoured structures. *Coastal Engineering*, 154:103572.

Dont, C. and Laborie, V. (2007). *CIRIA, CUR, CETMEF, (2007), The Rock Manual. The use of rock in hydraulic engineering (2nd edition). C683, CIRIA, London, ISBN 978-0-86017-683-1.*

Fredsøe, J., Deigaard, R., et al. (1992). *Mechanics of coastal sediment transport*, volume 3. World Scientific.

Frostick, L. E., McLelland, S. J., and Mercer, T. G. (2011). *Users guide to physical modelling and experimentation: Experience of the HYDRALAB network*. CRC Press.

Hoffmans, G. (2012). *The Influence of Turbulence on Soil Erosion*. Deltares select series. Eburon.

Hoffmans, G. J. and Verheij, H. J. (1997). *Scour manual*, volume 96. CRC press.

Hughes, S. (1993). *Physical Models and Laboratory Techniques in Coastal Engineering*. Advanced series on ocean engineering. World Scientific.

Kalf, P. (2013). Winnowing sub-surface entrainment of particles.

Mangor, K. (2020). Statistical description of wave parameters. `http://www.marinespecies.org/introduced/wiki/Statistical_description_of_wave_parameters`. Online; accessed 30 June 2020.

Medina, J. and Gómez-Martín, M. (2016). *Cubipod® Manual 2016*.

Nelson, R. C. (1994). Depth limited design wave heights in very flat regions. *Coastal Engineering*, 23(1-2):43–59.

O'Donoghue, T., Doucette, J., van der Werf, J., and Ribberink, J. (2006). The dimensions of sand ripples in full-scale oscillatory flows. *Coastal Engineering*, 53(12):997 – 1012.

Papadopoulos, D. (2012). *Scour below the toe of breakwaters: Investigation of scour formation through a geometrically open filter configuration located at the toe of a rubble mound breakwater lying upon sand*. PhD thesis.

Schiereck, G. and Verhagen, H. (2012). Introduction to bed, bank and shore protection 2nd edition.

Shields, A. (1936). Anwendung der aehnlichkeitsmechanik und der turbulenzforschung auf die geschiebebewegung. *Mitteilungen der Preussischen Versuchsanstalt für Wasserbau und Schiffbau*, Berlin no 26.

Simm, J. D., Brampton, A., Beech, N., and Brooke, J. (1996). *Beach management manual*. CIRIA London.

Sumer, B. M. and Fredsøe, J. (2000). Experimental study of 2d scour and its protection at a rubble-mound breakwater. *Coastal Engineering*, 40(1):59–87.

Tulsi, K. (2016). *Three dimensional method for monitoring damage to dolos breakwaters*. PhD thesis.

Van der Meer, J. (2002). Technisch rapport golfoploop en golfoverslag bij dijken. *TR33*.

Van der Meer, J. W. (1998). Application and stability criteria for rock and artificial units. *Dikes and revetments, Rotterdam/Brookfield: AA Balkema*, pages 191–215.

van Gent, M. R. and van der Werf, I. M. (2014). Rock toe stability of rubble mound breakwaters. *Coastal Engineering*, 83:166 – 176.

Van Rijn, L. C. and Kroon, A. (1993). Sediment transport by currents and waves. In *Coastal Engineering 1992*, pages 2613–2628.

Xie, S.-L. (1981). Scouring patterns in front of vertical breakwaters and their influences on the stability of the foundation of the breakwaters.

Appendix A

Material armour layer and toe structure

For practical reasons, the same stones are used for the toe structure and the armour layer. Normally this would lead to problems, since the armour layer grading has to be larger than the grading of the toe structure. In this research, a rigid breakwater is made and the armour layer can consists of smaller stones. These stones are glued together and can not become unstable as a normal rubble mound structure slope. On the other hand, the toe structure does need to be stable since it is constructed in a standard manner. The considerations and assumptions made for the choice of the material are listed below:

- The toe structure and the breakwater are constructed out of the same grading.
- The toe structure has to be stable following the standard stability equations.
- The grain size of the toe structure can not be much larger than needed, since this would cause problems with the filter layer.
- The stones can not be to big since it is assumed by the fluid dynamics laboratory that bigger stones are more difficult to glue together.
- The grading has to be equal to or smaller than the stability criteria for the armour layer. Bigger stones would create a rougher slope, this could underestimate the return flow and the scour.
- The grading has to be easily available at the partners of the fluid dynamics laboratory.

It is decided to choose a grain size which is close to, but larger than, the needed grain size for toe stability. In this way the least amount of practical problems occur in the physical model. For toe stability multiple stability criteria can be used, which are valid for different hydraulic conditions. The stability criteria by van Gent and van der Werf (2014) is valid for all the used hydraulic conditions in this research. Therefore, van Gent is used to determine the stability of the toe structure. Van Gent is valid when the following criteria hold:

- h_t / h = 0.7 - 0.9
- h / H_s = 1.2 - 4.5
- h_t / d_{n50} = 7 - 25

Van Gent relates the grain size to the number of damage (N_{OD})of the toe structure, eq. (A.1). For this research, no damage is allowed. The N_{OD} has to be smaller than 1 for this requirement. In fig. A.1, the final used grading can be found and in table A.1, the calculation for the toe stability. The expected N_{OD} is equal to 0.32 and is this well within the required limits.

$$d_{n50} = 0.32 \cdot \frac{H_s}{\Delta \cdot (N_{OD})^{\frac{1}{3}}} \cdot \left(\frac{W_t}{H_s}\right)^{\frac{1}{3}} \cdot \left(\frac{\left(\frac{\pi \cdot H_s}{T_{m-1,0}} \cdot \frac{1}{\sinh k \cdot h_t}\right)}{\sqrt{g \cdot H_s}}\right)^{\frac{1}{3}} \tag{A.1}$$

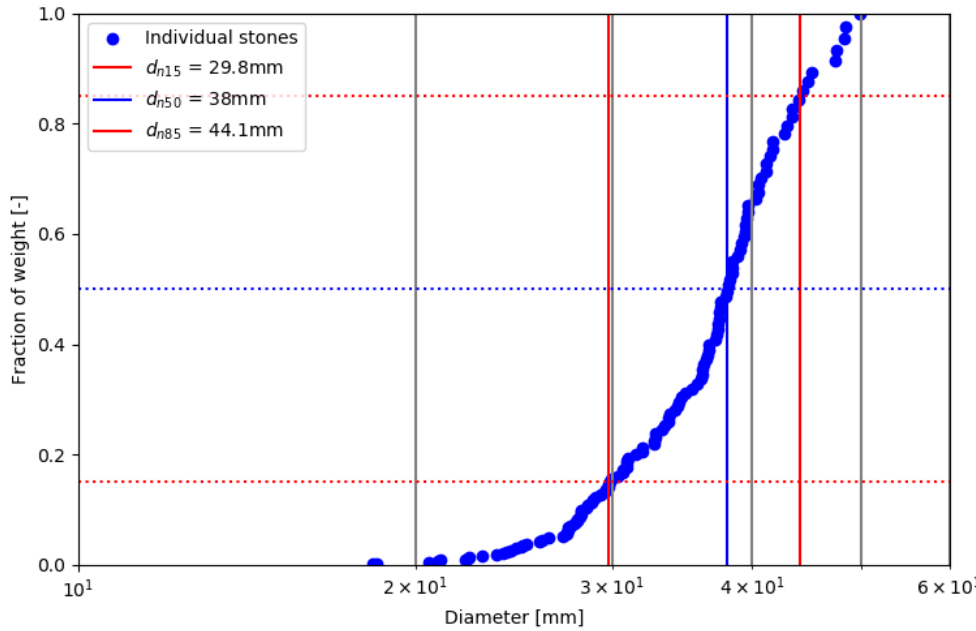

Figure A.1: Grading armour layer and toe structure.

For the armour layer stability Van der Meer (1998) is used to determine the needed d_{n50}. The van der Meer equation relates the damage number (S_d) to the hydraulic conditions and armour layer dimension. Initial damage occurs for $S_d = 2$, thus that value is chosen for this research. eqs. (A.2) to (A.5) are used and the maximum number of waves for these formulas is 7500. If the breaking parameter (eq. (A.2)) is larger than the critical breaking parameter (eq. (A.3)), the formula for surging waves (eq. (A.5)) is used. On the other hand, if the breaking parameter is smaller than the critical value, the formula for plunging waves (eq. (A.4)) is used. The needed d_{n50} according to the van der Meer equation is equal to $0.089m$. The used d_{n50} is much smaller, but with all the considerations and assumptions made this is not a problem. It should be noted that a small over estimation of the scour can be caused by this, since the slope is smoother.

$$\xi = \frac{\tan\alpha}{\sqrt{\frac{2\pi H_s}{g T_p^2}}} \tag{A.2}$$

$$\xi_{critical} = \left(6.2P^{0.31}\sqrt{\tan\alpha}\right)^{\frac{1}{P+0.5}} \tag{A.3}$$

$$\frac{H_s}{\Delta d_{n50}} = 6.2P^{0.18}\left(\frac{S_d}{\sqrt{N}}\right)^{0.2}\xi^{0.5} \rightarrow \text{For plunging waves} \tag{A.4}$$

$$\frac{H_s}{\Delta d_{n50}} = 1.0P^{-0.13}\left(\frac{S_d}{\sqrt{N}}\right)^{0.2}\sqrt{\cot\alpha}\,\xi^{P} \rightarrow \text{For surging waves} \tag{A.5}$$

Parameter	Unit	Value
d_{n50}	$[m]$	0.038
H_s	$[m]$	0.18
Δ	$[-]$	1.56
W_t	$[m]$	0.19
$T_{m-1,0}$	$[s]$	2.5
k	$[1/m]$	0.64
h_t	$[m]$	0.323
g	$[m/s^2]$	9.81
$\boldsymbol{N_{OD}}$	**$[-]$**	**0.31**

Table A.1: Calculation toe stability.

Parameter	Unit	Value
S_d	$[-]$	2
N	$[-]$	7500
P	$[-]$	0.4
α	$[degrees]$	26.57
Δ	$[-]$	1.56
H_s	$[m]$	0.18
T_p	$[s]$	2.5
g	$[m/s^2]$	9.81
$\boldsymbol{d_{n50}}$	**$[m]$**	**0.089**

Table A.2: Calculation armour stability.

Appendix B

Sand properties

The sand which is used in the sandpit has a d_{n50} of $0.26mm$ and the grading curve can be found in fig. B.1. For the scale model, sand with a small grain size is often used. This is to have an as large as possible scaling factor, without distorting the geometric scale. The smallest d_{n50} for sand is approximately $0.15mm$. Both mentioned gradients are suitable for this research, but they do behave slightly different. Both these gradients are considered for these experiments and there are two main differences.

First of all the smaller grain size leads to a larger maximum scaling factor. As discussed in section 2.4.3 sand has a grain sizes between $0.062mm$ and $2mm$. For the smaller grain distribution a maximum scaling factor of 10 can be reasonable, but for the larger distribution this is not possible. If the larger sand is scaled, the scaled material falls in the grain size range of gravel. The scaled material would not behave similar, which is thus not realistic. On the other hand, in the used flume a typical scaling factor would be at least 10. So for most prototypes, the sand used can not be correctly scaled independent of the chosen scale model sand.

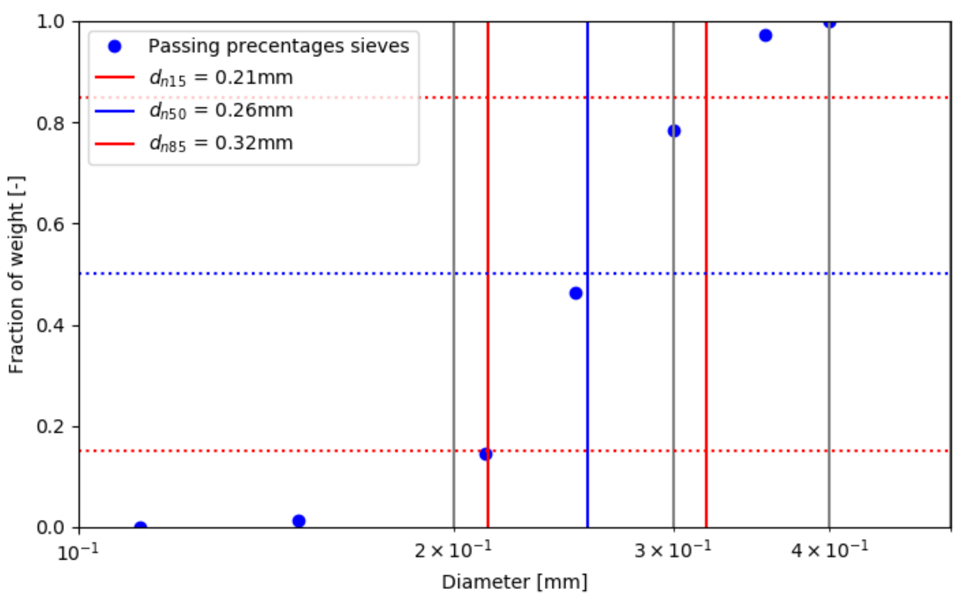

Figure B.1: Grading sand layer.

The second difference between the two grain sizes lies in the the mode of transport. Sand can be in suspended load transport, bed load transport or both. The mode of transport can be determined by the dimensionless Rouse number as shown in eq. (B.1). This is described by Borsje et al. (2014), in which the sediment fall velocity described by Van Rijn and Kroon (1993) is used. For the used hydraulic conditions in this research the Rouse number is mostly between 2 and 3.5 for the used sediment ($d_{n50} = 0.26$). Fredsøe et al. (1992) defined three regimes for the transport mode:

- P < 1.2 Suspended load transport
- 1.2 < P < 2.5 Both suspended load and bed load transport
- 2.5 < P Bed load transport

So for this research only the biggest waves cause suspended transport. When smaller sediment ($d_{n50} = 0.15$) is used the Rouse number lies between 1 and 2. Thus, indicating more suspended transport and possibly other scour behaviour.

$$P = \frac{w_s}{\kappa u*} \tag{B.1}$$

To conclude, the smaller sand is slightly more suitable for scaling back to full scale. Besides that it gives possibilities to research suspended load transport. On the other hand, the larger sand is use full to research bed load transport. The influence of the chosen sand can be best described by using multiple grain distributions. For this research, the smaller sand was due to practical reasons not available at the time of the experiments. Thus, the sand with ($d_{n50} = 0.26$) is used and for further experiments it is use full to compare this with the smaller sand ($d_{n50} = 0.15$).

Appendix C

Design rigid breakwater

The rigid breakwater/ rubble mound structure which is used for the research, is made in the fluid dynamics laboratory. It is constructed in order to work more efficiently while doing experiments. To achieve this the breakwater must be easy to use and saving preparation time when comparing to loose lying rocks. A big advantage would be that, in between tests, the breakwater does not need to be rebuild. The breakwater will also be used for other experiments in the laboratory and the main requirements which need to be considered are listed below:

- The breakwater must be permeable on all sides.
- The breakwater must be solid, strong and stiff.
- The breakwater must be capable of being lifted by a crane.
- The breakwater must be able to be used for several types of tests in the fluid dynamics laboratory.
- The breakwater must be clean to prevent turbid water.
- The maximum width of the breakwater is $0.78m$, so that it can be placed inside the wave flume without damaging it.

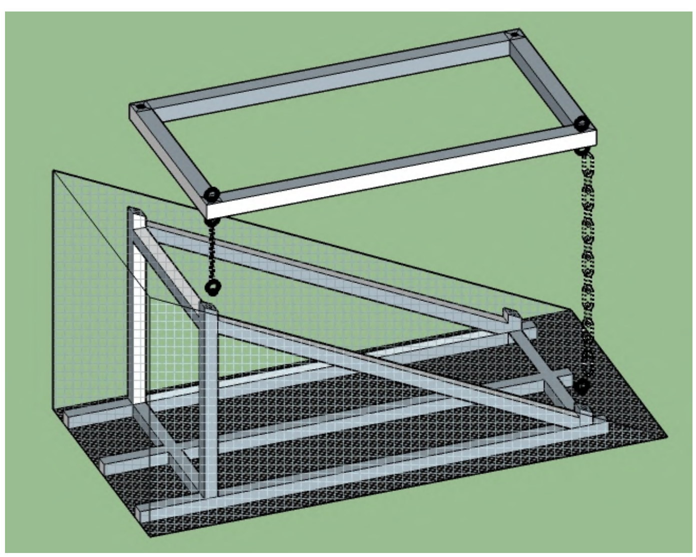

Figure C.1: Steel frame rigid breakwater.

To achieve these requirements a breakwater is built inside a mold on a permeable steel plate and around a steel frame, fig. C.1. This frame can be lifted by a custom made lifting frame to avoid transverse forces. Earlier made rigid breakwaters had the tendency to crumbling stones due to bending of the frame. The use of the lifting frame prevents this as much as possible. The stones used for the breakwater are cleaned before they are mixed with epoxy in the concrete mixer. When covered with epoxy, the stones are thrown into a mold in which the steel frame fits perfectly. In fig. C.1 the drawing of the frame and the surrounding mold (transparent pattern) are shown. The bottom plate (black in the figure) is made out of perforated steel to keep every side of the breakwater permeable.

In fig. C.2 the breakwater can be seen just after the stones were mixed with the epoxy and thrown into the mold. After this it had to dry for a few days before it was taken out. The final product can be seen in fig. C.3. The dimensions of the breakwater are:

- Width: $0.78m$
- Length: $1.60m$
- Height: $0.75m$

Figure C.2: Rigid breakwater after all the stones are thrown in to the mold.

Figure C.3: Rigid breakwater while hanging in crane

Appendix D

Bed protection

As described in section 3.2.2, three aspects are important to consider for the bed protection. First of all the bed protection has to be stable under the incoming waves. For this the Shields criteria for waves is used, described in section 2.1.2. The bed protection material is basalt, because it has a high density. This to make it more stable without needing a large grain size. A smaller grain size decreases the possibility of winnowing. It was found that for this research the d_{n50} must be at least $6mm$ for the initial chosen significant wave height (H_s) of $0.14m$ and peak period (T_p) of $1.6s$. For the largest H_s ($0.18m$) and longest T_p ($2.5s$) which can be tested in the flume, the d_{n50} must be at least $10mm$.

However, to also satisfy other criteria a grain size with a d_{n50} of approximately $8mm$ is chosen. If the higher waves would induce to much motion, a slightly lower wave could be used. After testing it turned out that the maximum H_s was $0.17m$ with a T_p of $2.5s$. For the used bed protection with a d_{n50} of $0.782mm$ this corresponds with a Shields factor of 0.055. The used grading can be seen in fig. D.1.

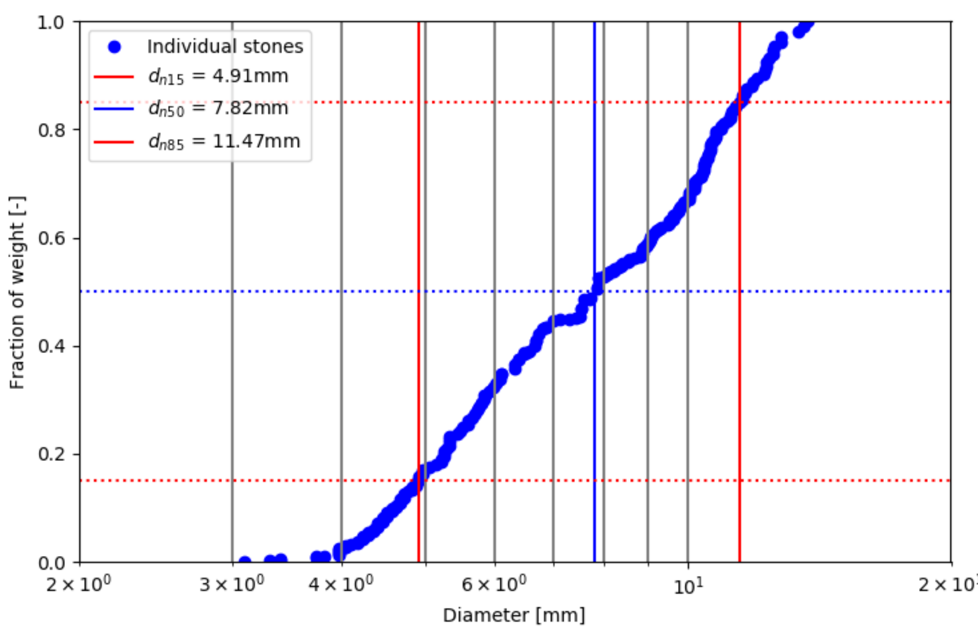

Figure D.1: Grading filter layer and bed protection.

The second requirement is that the bed protection is stable as a filter under the toe structure. For this the stability between the two layers, the internal stability and the permeability are considered. For a closed filter, the stability criteria are related to the grain sizes. The three criteria, described by Schiereck and Verhagen (2012), are listed below and are all satisfied:

- Stability: $\frac{d_{n15armour}}{d_{n85filter}} < 5 \longrightarrow \frac{d_{n15armour}}{d_{n85filter}} = \frac{29.8}{11.47} = 2.6$
- Internal stability: $\frac{d_{n60armour}}{d_{n10filter}} < 10 \longrightarrow \frac{d_{n60armour}}{d_{n10filter}} = \frac{9.1}{4.6} = 2.0$
- Permeability: $\frac{d_{n15armour}}{d_{n15filter}} > 5 \longrightarrow \frac{d_{n15armour}}{d_{n15filter}} = \frac{29.8}{4.91} = 6.1$

For the final requirement, winnowing can not occur trough the bed protection on the sand. For this similar criteria can be used as for a closed filter. However, the sand is so small that these criteria can not be satisfied. The layer can still be stable if the layer would satisfy the open filter layer criteria. In this case the critical hydraulic gradient needs to be smaller than the actual hydraulic gradient. This can be achieved by increasing the thickness of the layer if the filter is not closed. For this criteria Kalf (2013); Hoffmans (2012) used fig. D.2 to determine the open filter stability.

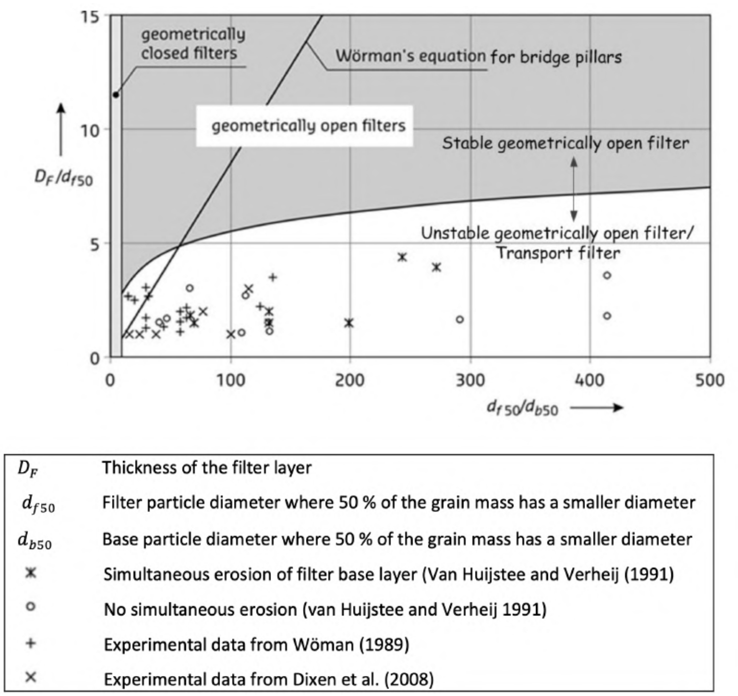

Figure D.2: Stability open filters. (Kalf (2013); Hoffmans (2012))

Appendix E

Test procedure

While doing experiments it is important to follow the same steps every test. This to keep the test as similar as possible. The followed test procedure is described in the list below.

- Flatten the sand bed and when needed supplement extra sand to the sandpit.
- Rebuild the filter layer and bed protection.
- Rebuild the toe structure.
- Fill the flume slowly with water from the reservoir.
- If necessary, flatten the sand bed at places where the water flow influenced the sand bed.
- Lower the laser sensors into the flume (Always same height!).
- Hang frame for laser sensor reference in the flume.
- Perform an initial measurement of the sand bed to use as reference.
- Raise the laser sensors out of the water! *
- Remove frame for laser sensor reference from the flume.
- Enter wave program into the computer program.
- Calibrate the wave gauges to 0 volt.
- Start measuring the waves (water elevation), at least one minute before the first wave for reference if needed.
- Start the interval capture with the different cameras.
- Start wave program and wait until finished.
- Stop the wave measurements.
- Hang frame for laser sensor reference in the flume.
- Lower the laser sensors into the flume (Always same height!).
- Perform an intermediate or final measurement of the sand bed. When doing an intermediate measurement, return to *.
- Remove frame for laser sensor reference from the flume.
- Drain the wave flume.
- Remove the bed protection and toe structure.

Appendix F

Physical model drawing with impermeable slope

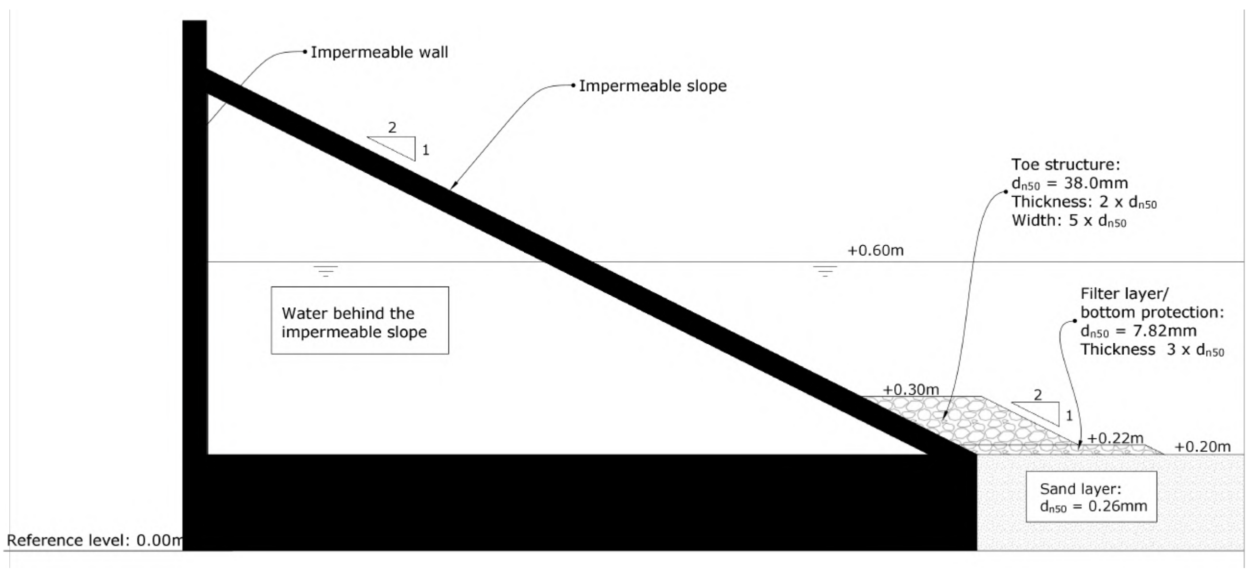

Figure F.1: Physical model with impermeable slope including used grain sizes

Appendix G

Wave conditions during testing

Test	H_{m0}	H_{max}	$T_{m-1,0}$	$T_{m2,0}$	K_R
A.1	14.2	23.7	1.49	1.36	0.50
A.2	14.4	23.2	2.21	1.84	0.67
A.3	14.4	28.3	2.26	1.86	0.66
A.4	14.6	23.2	2.20	1.88	0.62
A.5	13.8	22.8	1.48	1.35	0.48
B.1	14.3	24.2	2.24	1.97	0.27
B.2	14.5	24.8	2.25	1.98	0.25
B.3	18.5	29.6	2.22	1.93	0.24
B.4	14.5	25.3	2.24	1.95	0.27
B.5	14.5	25.4	2.24	1.95	0.27

Table G.1: Incoming offshore wave conditions.

Test	H_{m0}	H_{max}	$T_{m-1,0}$	$T_{m2,0}$	K_R
A.1	12.1	19.3	1.50	1.35	0.63
A.2	13.5	23.0	2.10	1.63	0.81
A.3	13.4	23.5	2.12	1.65	0.78
A.4	13.5	22.3	2.13	1.66	0.77
A.5	12.2	19.3	1.51	1.36	0.61
B.1	13.9	24.1	2.63	1.68	0.43
B.2	13.9	21.8	2.57	1.74	0.40
B.3	17.1	23.8	2.77	1.65	0.43
B.4	14.0	25.5	2.62	1.72	0.42
B.5	14.0	25.5	2.62	1.72	0.41

Table G.2: Incoming wave conditions.

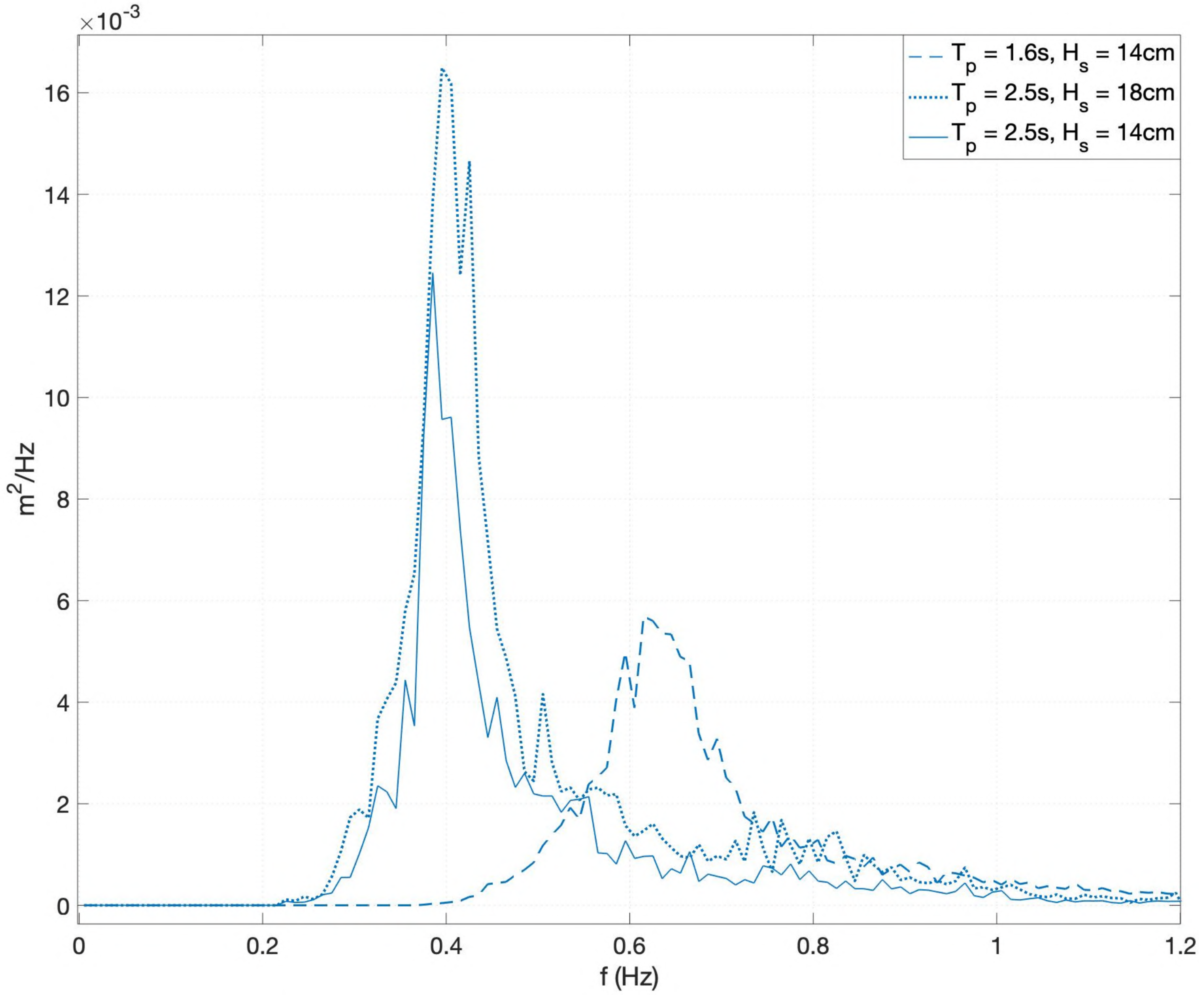

Figure G.1: Incoming offshore wave conditions.

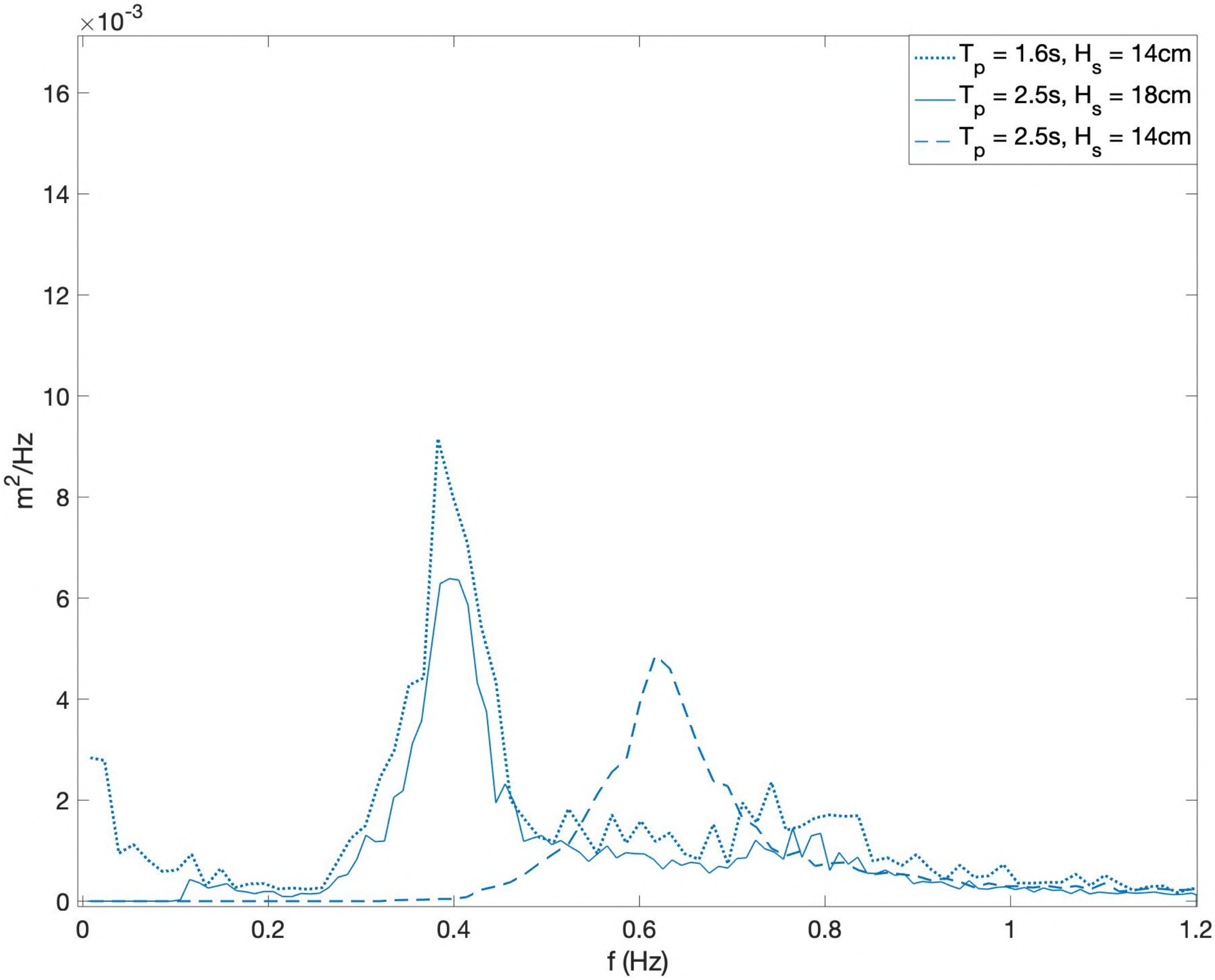

Figure G.2: Incoming wave conditions.